NONSTRANGE BARYON RESONANCES

Chairman	A. Lagarrigue
Rapporteur	R. Plano
Discussion leaders	A. Donnachie
	J. Mulvey
Secretaries	A. Kravtsov
	V. Koptev
	V. Grischin
	E. Kistenev
	B. Yuldashev

NONSTRANGE BARYON RESONANCES

R. Plano

I. Introduction

This report will discuss the experimental status of the nucleon resonances concentrating on developments since those reported by Donnachie [1] and Rushbrooke [2] at Vienna with the major emphasis on results since the Lund Conference [3]. This material breaks naturally into formation experiments and production experiments.

The production experiments were concerned almost entirely with $N\pi\pi$ decays of resonances in the 1400—1700 *MeV* mass region, including questions of mass and width values, Δ (1236) π and ΛK branching ratios, attempts at spin-parity analysis, and identification with the N^*'s known from elastic phase shift analyses. Almost all these problems have eluded experimental agreement. This is due in part to the fact that the interpretation of these production experiments and their correlation with phase shift analysis is unclear in principle, given the impossibility of meaningfully subtracting background with the currently available theoretical understanding and experimental data.

The formation experiments have confirmed the twelve well established nucleon resonances discussed by Donnachie at Vienna [1] with only minor changes in their parameters, strengthened a few of the doubtful candidates while removing none of them, and added several new candidates at higher mass with good evidence.

In summary, the experimental status of nonstrange baryon resonances has not changed greatly since the spurt given by the πN elastic phase shift analyses of CERN, Saclay, and Berkeley reported by Lovelace [4] at the Heidelberg Conference three years ago. New data of high quality and in large quantities is desperately needed to motivate and inspire as well as to constrain and severely test theoretical ideas. This is well illustrated by the fact that a recent and quite different fit [5] to the **squares** of the baryon masses gave reasonable agreement with the data.

The authors wisely point out that only further research can decide whether the regularities observed are real or «the result of numerical accidents in the limited data available».

It is perhaps worth noting that although the roughly 50 baryon states now catalogued, of which the major quantum numbers are known for about 35, represent an impressive experimental achievement, the previous spectroscopies had acquired vastly more data of high quality before an adequate understanding was attained. There is every reason to expect that the leap in understanding required here will not be trivial, but rather at least comparable to that which led to a reasonably complete description of atomic spectra.

II. Formation Experiments

Before discussing the recent developments in elastic phase shift analysis, I would like to review the basic ideas, comment on the extraction of resonance parameters with errors from Argand plots, and remark on the problems in correlating these results with results from production experiments. Since I have never worked seriously on an elastic phase shift analysis, these comments are those of an outsider and have been gleaned from extensive discussions with many experts in the field [6].

An informal discussion was held at the Lund Conference [3] including representatives of all major groups doing elastic phase shift analyses to consider the problems of extracting resonance parameters and realistic errors on these parameters from Argand diagrams. The general consensus was that a precisely defined and rigorously correct procedure cannot be given, but that the general procedure as outlined below is easily described and should permit any interested physicist to extract his own estimates. In view of these difficulties, the Particle Data Group [7] now presents a range of masses and widths from various fits rather than some average. These ranges should not be mistaken for errors in the sense of standard deviations. My own guess, which was not contradicted by any phase shift analyst I was able to talk to, is that typical errors in mass range from 50 to 200 MeV and uncertainties in width range upwards from 50% although some of the well established resonances (notably the Δ (1236)) have much better determined parameters.

The major conceptual difficulty arises from the presence of background whose changes in elasticity and phase under a resonance are difficult to separate from the resonance with currently available theoretical models and statistics. It is generally assumed that the resonance and background contributions multiply in the S matrix so the total amplitude has a phase given by the sum of the phases and an elasticity given by the product of the elasticities of the background and the resonance.

Although the detailed nature of the background is in general unknown, the properties of a pure Breit — Wigner as illustrated in Fig. 1 are simple. For a

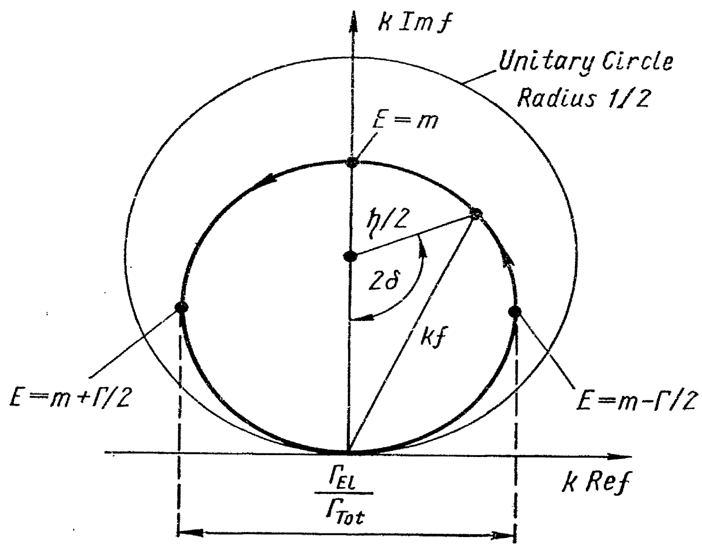

Fig. 1. The properties of a simple Breit — Wigner amplitude on an Argand diagram in the absence of background. The relationships between the amplitude and the elastic, inelastic and total cross sections are also shown. k is the CM momentum.

simple Breit — Wigner in the absence of background, the amplitude describes a counterclockwise circle as the energy increases. The central mass occurs at:

1) the point of maximum speed $|df/dE|$. This is the most commonly used criterion as it is reasonably convenient to extract from an Argand plot and as the background seems to be most nearly constant in this parameter;
2) the minimum elasticity (maximum σ_{inel});
3) a phase of 90° (or 0° if $\Gamma_{el}/\Gamma_{tot} < {}^1/_2$);
4) the maximum $|f|$ (maximum σ_{el});
5) the maximum Im f (maximum σ_{tot}).

In the absence of background all five criteria give the same result, but with moderate and common amounts of background, the five criteria can give quite different parameters as illustrated in Fig. 2*a*. Note that the maxima in σ_{el}, σ_{tot}, and σ_{inel} occur at considerably different energies and that the point of maximum speed may well occur at yet another mass value. This situation approximates that of the P_{11} (1470) for which the maximum speed is at about 1470 *MeV*, maximum $|f|$ at 1450 *MeV*, maximum Im f at 1500 *MeV*, and minimum elasticity at 1600 *MeV*. All these numbers are very rough guesses, but I believe realistically indicate the problem.

The wide spread between the maximum in σ_{el} and σ_{inel} is of particular interest in attempting to correlate the production experiments showing $N\pi\pi$ bumps in the 1470 *MeV* region with the P_{11} (1470). The correlation is even more obscure as the background in the production reaction may be quite different from that in elastic scattering. Therefore a bump in a production experiment mass distribution may be due to a resonance observed in an elastic phase shift analysis even though the central masses differ by many standard deviations.

Fig. 2*b* illustrates an even more vicious and unpleasant example in that σ_{inel} exhibits no peak whatsoever although the Argand diagram shows a clear resonance using the criteria of σ_{el}, σ_{tot} or maximum speed.

It should be clear that similar difficulties arise in extracting the width and the elastic branching ratio and that the uncertainties are even larger in these cases.

To balance these comments, it should be emphasized that the well established resonances (those with an appreciable elastic branching ratio and not too pathological background) have shown remarkable stability over the past three years in spite of considerable controversy. It is also clear that production experiments must be analyzed more carefully including detailed fits to background and resonances with interference effects included.

A. Elastic Phase Shift Analyses. Data relevant to πN elastic phase shift analyses which was submitted to this conference is summarized in Table 1. These data

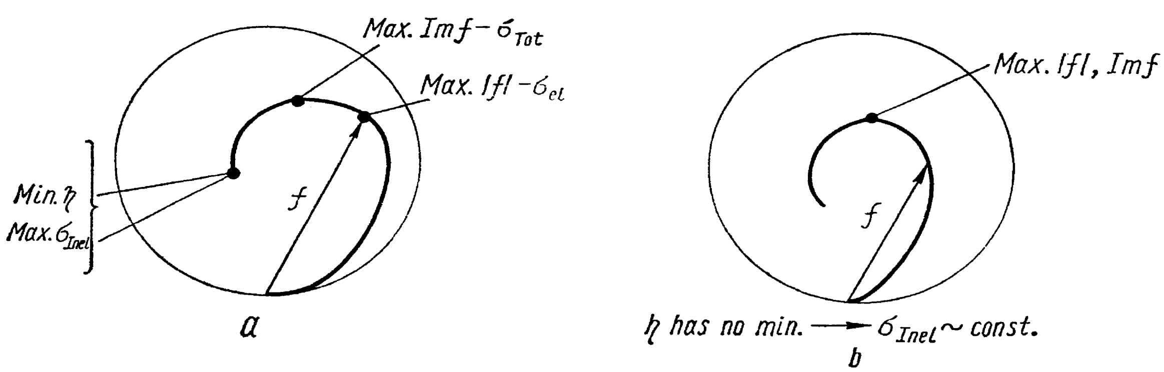

Fig. 2. Possible amplitudes exhibited on Argand diagrams to illustrate difficulties in extracting resonance parameters. (*a*) An approximation to the P_{11} wave. The criterion of maximum speed yields a fourth estimate for the central mass. (*b*) A pathological case in which the inelastic cross section shows a smooth behavior although a resonance is clearly visible on the Argand diagram.

include measurements of total cross sections, differential cross sections (DCS) including one measurement restricted to backward scattering (DCS (π)), and polarization measurements (POL). All new measurements show general agreement with the main features of published phase shift analyses, but there are areas of strong

Table 1

New Data on $\pi N \to \pi N$

Reaction	Technique	Measured	E_{cm}	Accuracy	Group	Ref.
$\pi^{\pm}p \to \pi^{\pm}p$ $\pi^{-}p \to \pi^{0}n$	CNTR	σ_{tot}	1.14—1.30 (13)	1/2%	Cavendish — Rutherford	[8]
$\pi^{-}p \to \pi^{0}n$	CNTR	DCS	1.22—1.51 (13)	3%	Princeton	[9]
$\pi^{+}p \to \pi^{+}p$	CNTR	POL + DCS	1.57—2.46 (24)	.03—5%	CERN	[10]
$\pi^{+}p \to \pi^{+}p$	CNTR	POL	1.60—1.98 (9)	.04	Rutherford	[11]
$\pi^{+}p \to \pi^{+}p$	CNTR	POL	1.98—2.29 (4)	.07	Argonne	[12]
$\pi^{-}p \to \pi^{-}p$	CNTR	DCS (π)	1.60—1.97 (15)	8%	College de France	[13]
$\pi^{-}p \to \pi^{-}p$	BC	DCS + σ_{tot}	1.4—2.0 (35)	6%	SLAC — LRL	[14]
$\pi^{+}p \to$ $\to \Sigma^{+}K^{+}$	BC	DCS + σ_{tot}	1.82—1.89 (2)	10%	LRL	[15]

disagreement. In general, $\pi^{-}p$ reactions are in satisfactory agreement whereas $\pi^{+}p$ reactions are less satisfactory. This is presumably due to the fact that less $\pi^{+}p$ data was available when the fits were made and is most apparent for backward $\pi^{+}p$ scattering on which very little information was previously available. A complete new fit is desirable to ascertain whether the new data will demand any radical changes in the accepted fits and, in any case, to obtain improved values of the parameters of the resonances.

A very high precision experiment [8] has been carried out by a Cavendish — Rutherford collaboration at the CERN Synchro-Cyclotron on πP scattering in the mass region 1.14—1.30 *GeV*. The purpose of the experiment was to obtain an order of magnitude improvement in the data available by measuring total cross sections to 0.5% and differential cross sections to 1.0%. As can be seen from Fig. 3, where the error bars vanish inside the dots, the experiment was successful. This paper reports on total cross sections only for $\pi^{\pm}p$ elastic scattering and $\pi^{-}p \to n\pi^{0}$ charge exchange scattering — the differential cross sections will be published shortly.

To obtain information on the nuclear interaction to the accuracy permitted by this data, corrections are required for the mixing of isotopic spin $^{1}/_{2}$ and $^{3}/_{2}$ states due to coulomb effects including interference and mass differences, and for the reactions

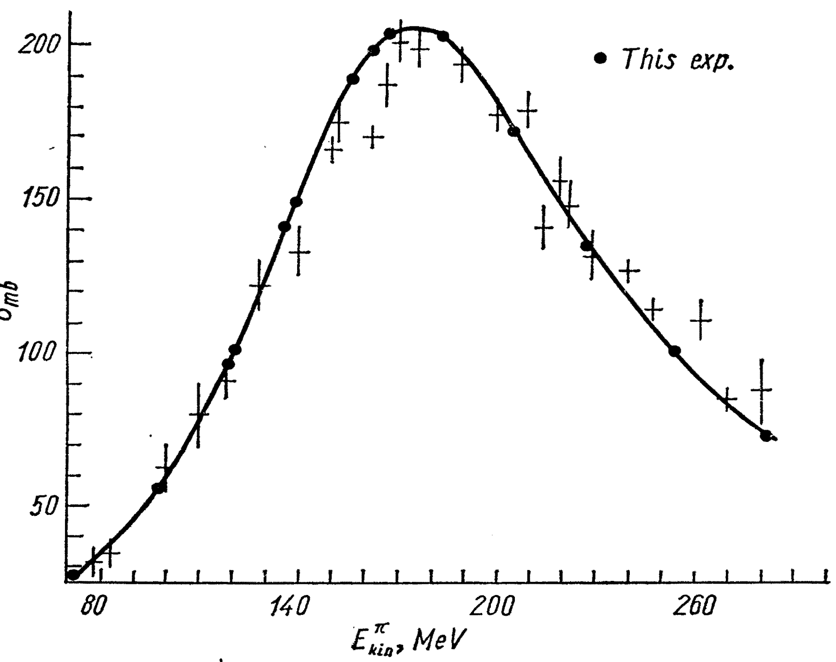

Fig. 3. The $\pi^{+}p$ total cross section as measured and fit by A. A. Carter et al. [8]. Selected earlier measurements are also shown.

$\pi^- p \rightarrow n\gamma$ (about 0.5 *mb*) and $\pi^- p \rightarrow n\pi^0\pi^0$ above 170 *MeV* (about 0.1 *mb*).

An estimate of the purely nuclear mass and width of the Δ (1236) was extracted giving for the Δ^{++}, (mass, width) = (1230.0 $\pm$ 0.6, 112.8 $\pm$ 3) and for the Δ^0, (1232.9 $\pm$ 0.6, 113 .6 $\pm$ 3). These errors are based on the experimental results and do not include the uncertainty in the approximately 1 *MeV* correction to eliminate coulomb effects. The mass of the Δ^{++} (1236) differs by more than 6 standard deviations from the accepted values of (1236.0 $\pm$ 0.6, 120 $\pm$ 2) [7]. This illustrates one difficulty in combining many imprecise experiments, none of which require detailed corrections, to obtain a «precise» result lacking required corrections.

It is worth noting that the mass difference $M(\Delta^0) - M(\Delta^{++}) = 2.9 \pm \pm 0.9$ *MeV* is consistent with a calculation of Socolow [16] based on tadpole and baryon-octet self energy diagrams which predicts 2.4 *MeV*. The previously accepted value [7] was 0.4 $\pm$ 0.9 *MeV*.

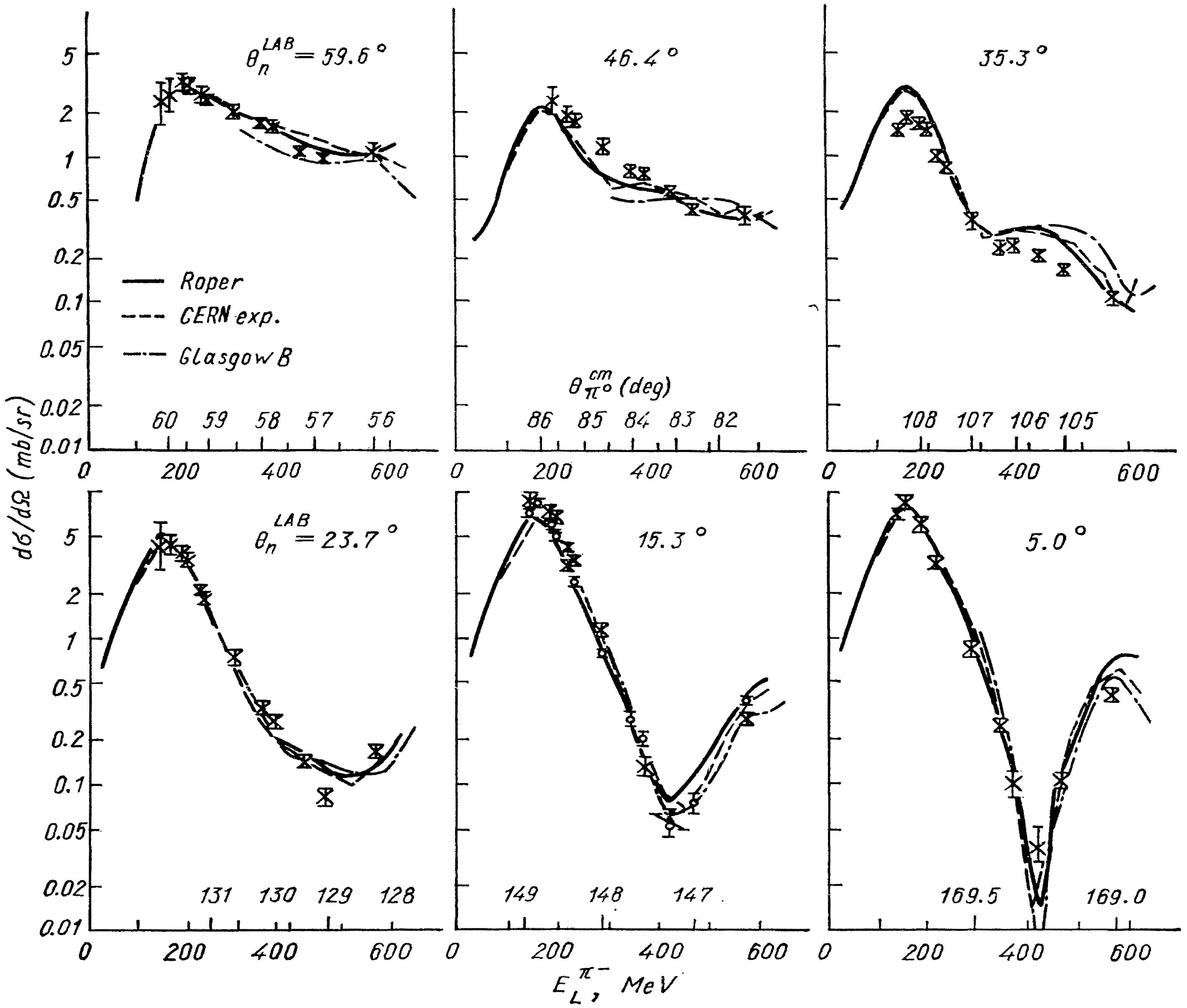

Fig. 4. Center of mass differential cross sections for $\pi^- p \rightarrow n\pi^0$. The phase shift fits of L. D. Roper et al. [75], CERN Experimental [21], and Glasgow (B) [22] are shown for comparison. K. Wendell Chen et al. [9].

A group at Princeton reported [9] on a careful measurement of $\pi^- p$ charge exchange scattering in the invariant mass region 1.22 — 1.51 *GeV* — a region in which very little data was previously available. The most striking feature of the data is a previously unobserved dip of three orders of magnitude near the backward direction at 1.40 *GeV*. This is explained as a cancellation of the imaginary parts of the P_{33} and P_{11} amplitudes combined with the destructive interference of the real parts of these amplitudes with the S and D wave background amplitudes. The spin flip amplitudes are negligible in the backward direction. The impressive agreement of the phase shift fits to this previously unknown feature as shown in Fig. 4 is good evidence for the basic validity of the elastic phase shift analysis.

Three measurements of polarization (POL) in $\pi^+ p$ elastic scattering in the invariant mass region 1.6 —2.5 *GeV* were submitted to the conference [10, 11, 12]. This is extremely useful data as previously only 17 polarization distributions for $\pi^+ p$ as opposed to 58 for $\pi^- p$ in the mass range of the CERN experiment [10] had been published. The data, which are of generally very high quality, are in reasonably good agreement among the three experiments as well as with older data. The apparatus used by the three groups was very similar including right and left counter hodoscopes to detect and isolate elastic scattering events and liquid filled Cerenkov counters in the region of kinematic ambiguity where the proton and pion are at equal angles in the laboratory. The polarized proton target material

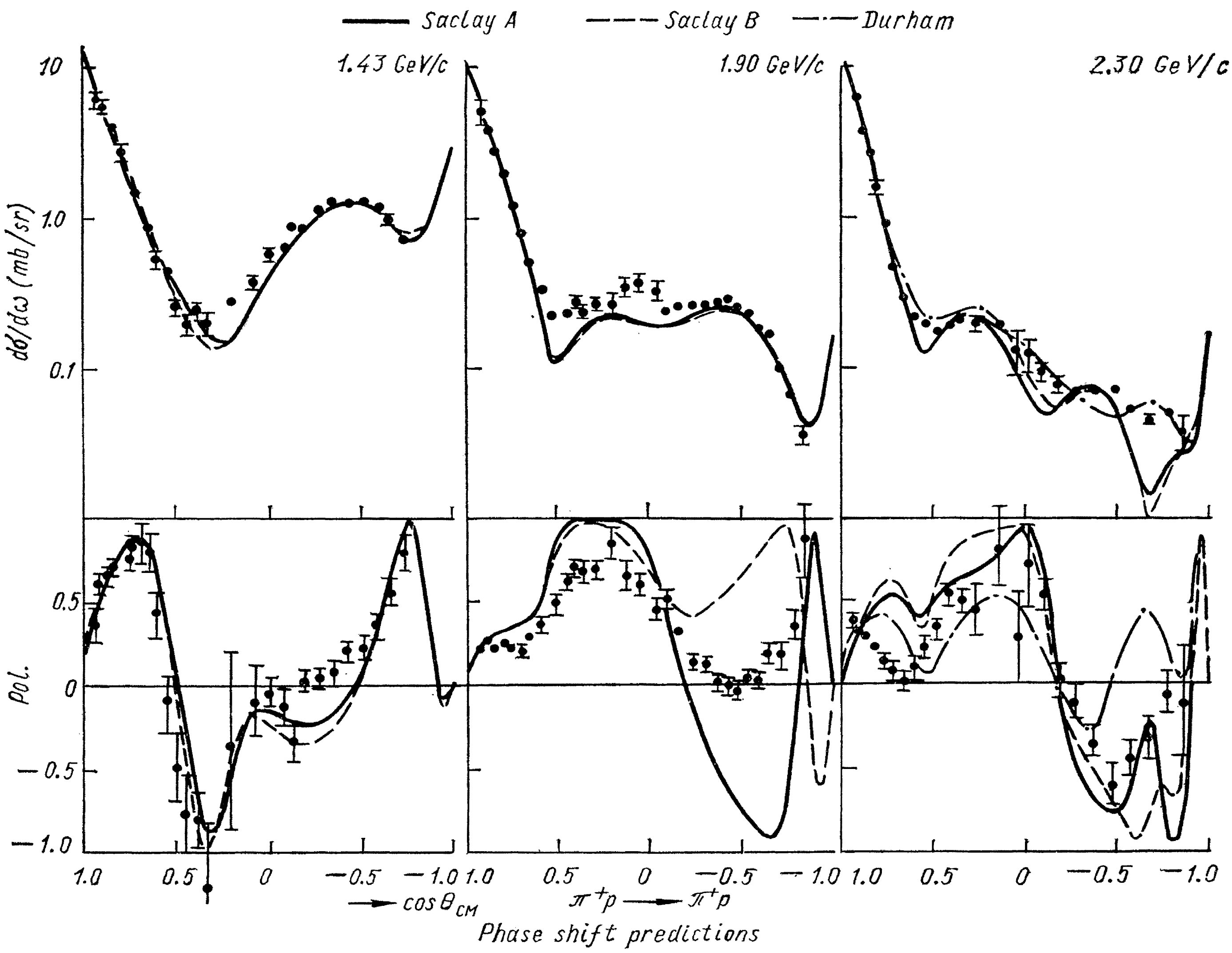

Fig. 5. The differential cross section and polarization of $\pi^+ p$ elastic scattering compared with the phase shift fits of Saclay [18] and Durham [19]. M. G. Albrow et al. [10].

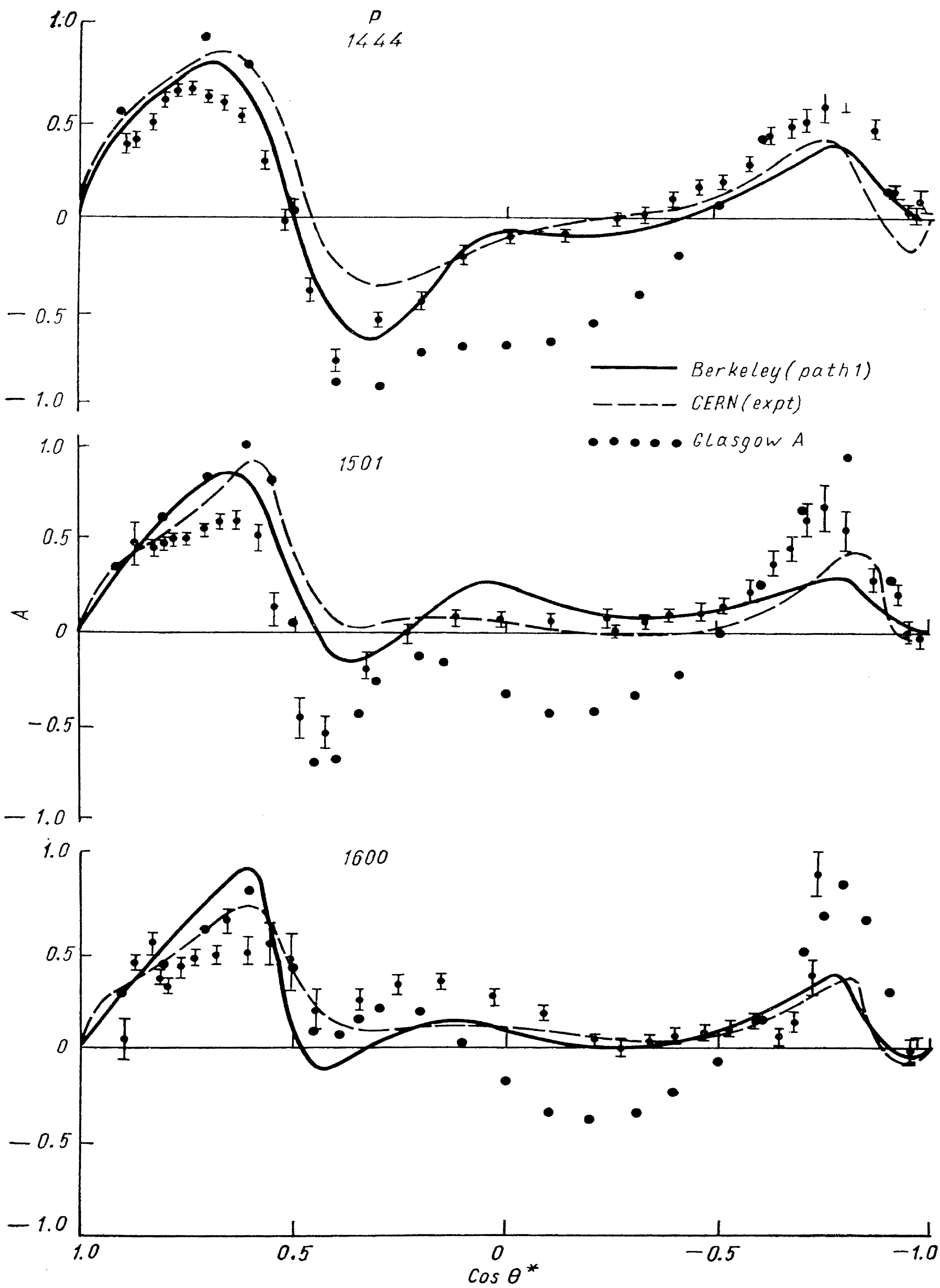

Fig. 6. Preliminary results for the asymmetry in π^+p elastic scattering at three of the nine momenta measured by R. M. Brown et al. [11]. The phase shift fits of Berkeley [20], CERN [21], and Glasgow [22] are shown for comparison.

used was butanol [10] with a polarization of 35±2%, Lanthanun Magnesium Nitrate (LMN) [11], and ethylene glycol [12] with a polarization of 40—45%.

The most complete and precise data are those of the CERN [10] contribution which includes measurements of differential cross sections as well as polarizations at 24 energies. Fig. 5 shows the data at three energies illustrating the good precision as well as some major features of the data noted by the authors. These include the forward peak and dips at t around —0.65 $(GeV/c)^2$ (presumably due to the ρ-trajectory passing through zero), $t \sim -2.8$ $(GeV/c)^2$ (first discussed by Booth [17]) and at $u \sim -0.15$ $(GeV/c)^2$, all of which were already well known. The polarization shows a known dip at $t = -0.65$ $(GeV/c)^2$ at higher momenta as well as a previously unnoticed minimum at $u \sim -0.65$ $(GeV/c)^2$ above 1.9 *GeV*. In general, both the DCS and POL show a rapidly varying behavior in the resonance region, while above 2.1 *GeV* the shapes remain fairly constant indicating the transition to the «asymptotic region» may be taking place.

Fig. 5 also shows predictions of the phase shift fits of Saclay [18] and Durham [19]. The agreement varies from reasonable to poor and clearly indicates a new fit should be made.

A Rutherford Laboratory group presented a preliminary analysis of about ¼ of the data obtained in a similar energy region [11]. Fig. 6 shows their data at three momenta and compares with the phase shift fits known as Berkeley (Path 1) [20], CERN (Experimental) [21], and Glasgow (A) [22] as reported in the compilation of Herndon et al. [23]. Again, the main features of the data are shown by all three fits, although the Glasgow (A) fit is in general worse than the other two,

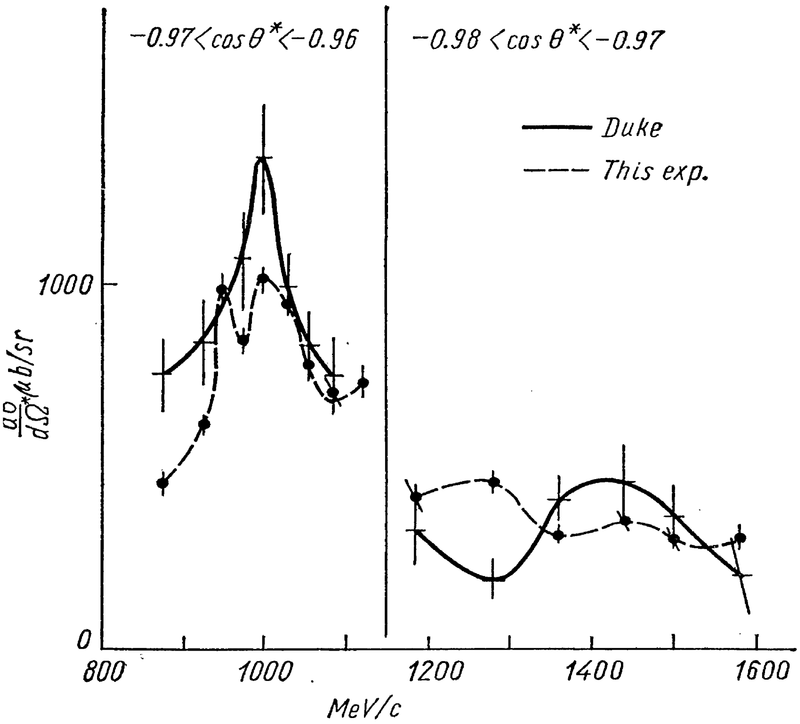

Fig. 7. $\pi^- p$ backward elastic scattering [13]. The earlier measurement of P. J. Duke et al. [25] is also shown.

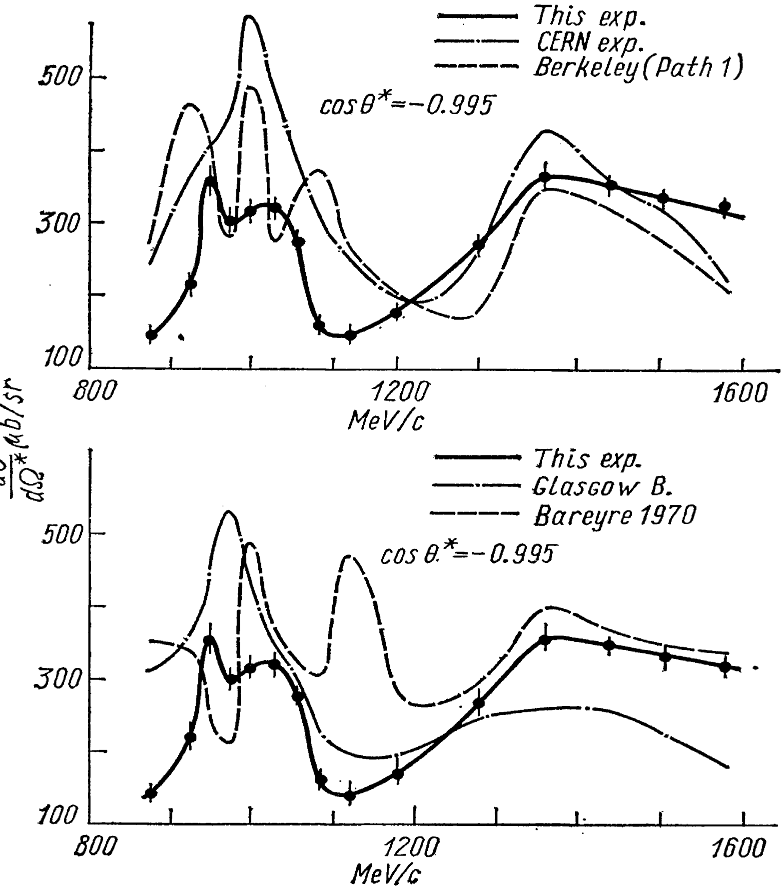

Fig. 8. $\pi^- p$ backward elastic scattering [13] compared with the phase shift fits of CERN [21], Berkeley [20], Glasgow [22], and Saclay [18], J. M. Abillon et al. [13].

and no fit follows the detailed behavior of the polarization in a thoroughly satisfactory fashion.

Similar preliminary data from an experiment done at Argonne National Laboratory at four momenta in this energy region [12] was presented. The features noted by CERN were also observed in this experiment and qualitative agreement with a Regge pole model of Berger and Phillips [24] was noted.

$\pi^- p$ elastic scattering in the backward direction ($-0.995 \leqslant \cos\theta^* \leqslant -0.955$) has been measured by a group at College de France [13]. Some of these data are shown in Fig. 7 where they are compared with similar data from a Rutherford Laboratory experiment [25]. The agreement is not good. Fig. 8 compares data from this experiment at $\cos\theta^* = -0.995$ with the phase shift fits known as CERN (Experimental) [21], Berkeley (Path 1) [20], Glasgow (B) [22], and Bareyre [18]. As might be expected from the experimental disagreement, there are large deviations from the phase shift fits.

Backward scattering is expected to be extremely sensitive to the phase shifts due to interference between the various waves combined with relatively small non-resonant amplitudes. A slight shift in the mass or width of a resonance can alter the backward differential cross section by a large amount. Conversely, these data should be highly effective in constraining resonance parameters and a new phase shift analysis is planned by this group [13].

An extensive bubble chamber study of $\pi^- p$ elastic scattering to obtain differential and total cross sections at 35 different energies in the invariant mass region 1.4—2.0 *GeV* has been carried out by a SLAC — LRL collaboration [14]. A total of about 80 *K* elastic events were analyzed as part of an extensive study of the $N\pi\pi$ channel yielding about 85 *K* inelastic events. The energy will be extended up to an invariant mass of 2.26 *GeV*. This large amount of data was measured on the Spiral Reader at LRL and carefully analyzed to minimize systematic errors due to such problems as short recoil protons.

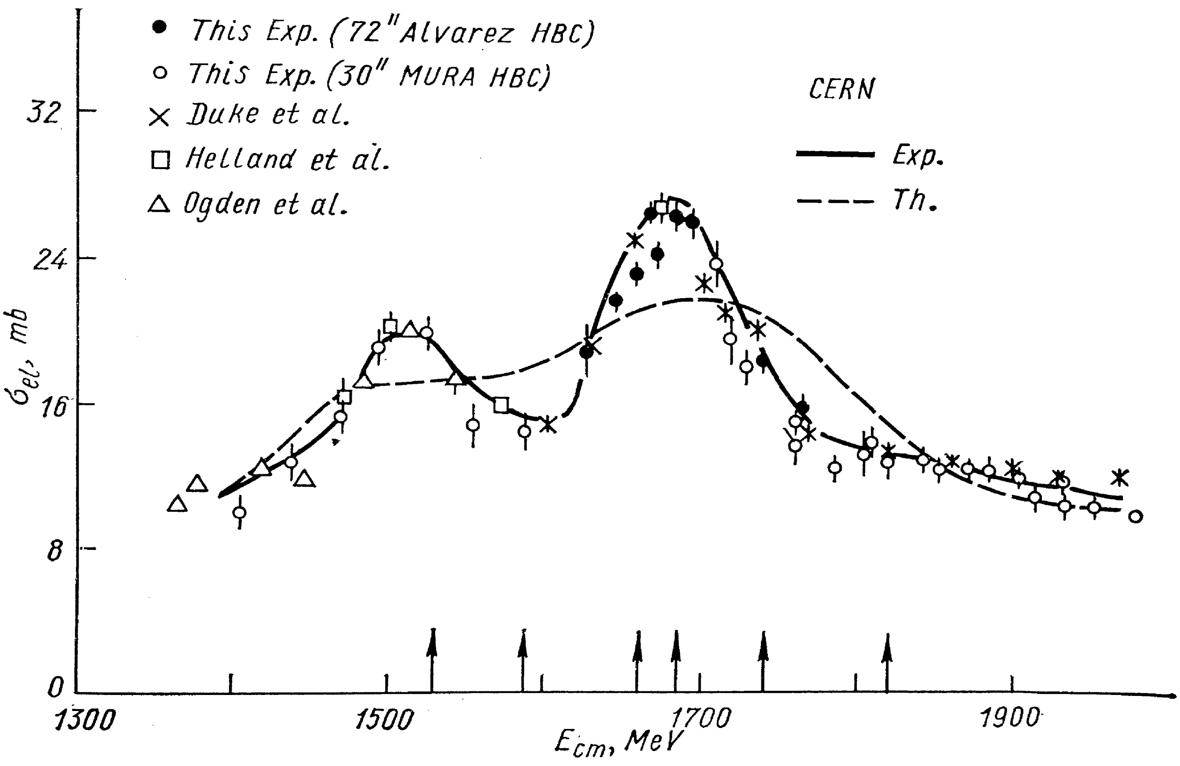

Fig. 9. $\pi^- p$ elastic cross section measurements of Brody et al. [14], Duke et al. [25], Helland et al. [26], and Ogden et al. [27] compared with the CERN phase shift fits [21]. A. D. Brody et al. [14].

To obtain total cross sections, the data were normalized to counter data in the region $-0.8 \leqslant \cos \theta^* \leqslant 0.7$, which region contributes only about 25% of the cross section, is slowly varying, and is relatively free from experimental biases for both the counter and bubble chamber work. The rapid variations in the cross section are then only weakly dependent on this normalization. Fig. 9 shows the resulting cross section together with the data of Duke et al. [25], Helland et al. [26], and Ogden et al. [27] together with the predictions of the CERN(Experimental) phase shift analysis [21] which, as the authors say, represents the data well. Fig. 10 shows differential cross sections at selected energies together with the predictions of the Saclay [28], Berkeley [29], and Glasgow [22] phase shift analyses, all of which represent the data fairly well.

A bubble chamber study of the two body inelastic channel $\pi^+p \rightarrow \Sigma^+K^+$ was reported by a LRL group [15]. The two momenta reported here were combined with seven momenta reported earlier [30] and the analysis repeated on the entire 1.85—2.09 *GeV* energy region, with no major change in the conclusions. Clear evidence is seen for the Δ (1950) in the $F37$ partial wave and the branching ratio to Σ^+K^+ remains at $2.0 \pm 0.4\%$ as in the previous analysis [30]. Some weak evidence is seen for other resonances, but the data are not convincing. Charge independence was also tested by means of triangle inequalities connecting this reaction with $\pi^-p \rightarrow \Sigma^0K^0$ and $\pi^-p \rightarrow \Sigma^+K^+$. One of the three triangle inequalities is slightly violated at $\cos \theta^* = +1.0$, but the violation is not statistically convincing.

In summary, the experimental data presented here shows a general agreement with existing elastic phase shift fits which helps to generate confidence in their overall validity. There are certainly non-negligible discrepancies which point out the need for a complete new fit to obtain improved resonance parameters, decide on the questionable candidates, and hopefully confirm the existence of new resonances.

One such new fit was reported by R. Ayed, P. Bareyre, and G. Villet [31]. This paper reported on an attempt to extract resonance parameters from a previously published [18] set of Argand diagrams based on data available through 1969. The total number of experimental data points used was 3150 and were fit with angular momentum states up to and including $l = 5$, which implied 44 free parameters to fit the data.

To obtain the Argand diagrams [18], the first step was to make independent fits at each of the 29 energies. These fits resulted in 5 to 20 solutions with a probability greater than 10^{-3} at each energy. The next step was to select one solution at each energy such that the amplitudes showed the smoothest behavior as a function of the energy. «Smoothest» was defined in terms of the minimum value of some function evaluated over all energies [20]. To test the influence of this function in rejecting or accepting resonances (all smoothness criteria tend to eliminate resonances), four different functions were tried — «minimal path», «minimum angle change», «minimal surface», and «minimal path at fixed momentum transfer». Somewhat surprisingly, the authors found that all methods gave solutions with the same general behavior.

To extract resonance parameters [31] from the resulting smoothed Argand diagrams, two parametrizations to combine background and resonance contributions were used. The first added the two contributions in the T matrix, while the second preserved unitarity by multiplying the two contributions in the S matrix. In both cases, the unitarized background amplitude was given by a power series in k — the *CM* momentum. As a further check on the effect of the parametrization of the resonances, the width was taken either as fixed or as variable while taking into account centrifugal barrier factors as well as threshold effects and relativistic corrections.

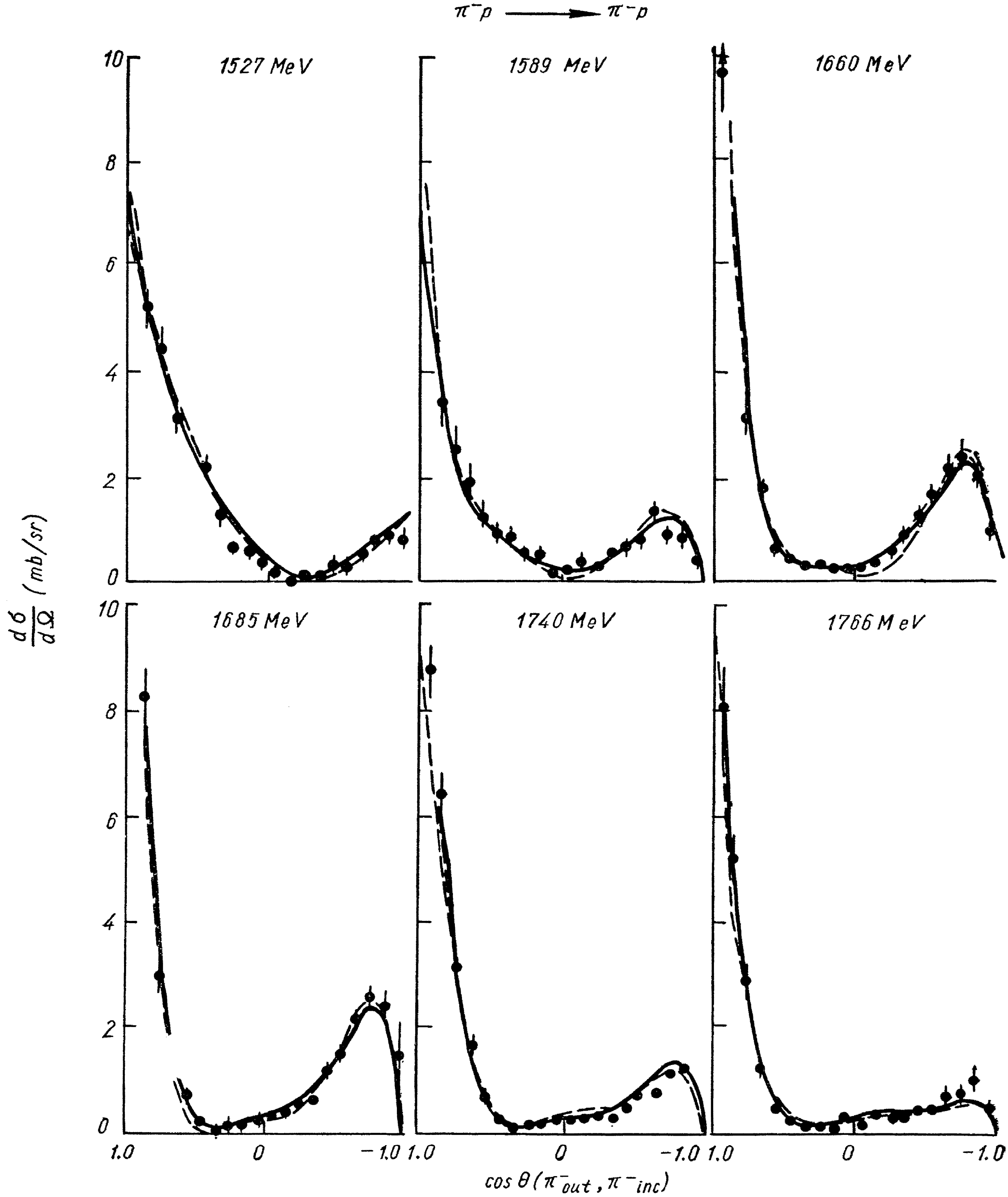

Fig. 10. π^-p elastic differential cross sections at several energies compared to the phase shift fits of Saclay [28], Berkeley [29], and Glasgow [22]. A. D. Brody et al. [14].

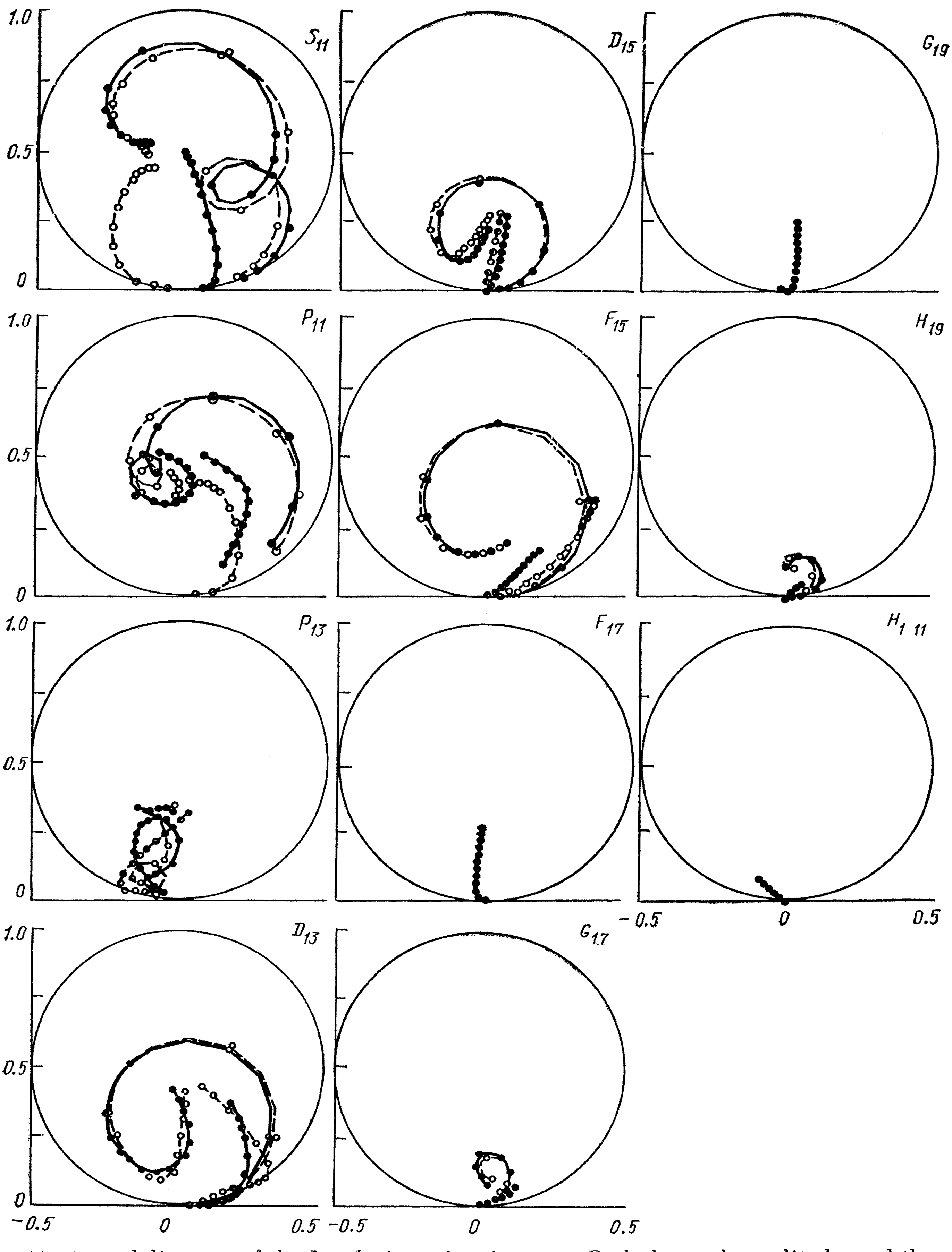

Fig. 11. Argand diagrams of the $I = 1/2$ isotopic spin states. Both the total amplitudes and the background amplitudes are shown. The solid lines refer to parametrization 1, which added background and resonance contributions in the T matrix, and the dashed lines refer to parametrization 2, which multiplied the two contributions in the S matrix. Energy dependent widths were used in both cases. Adjacent points are separated by 50 MeV in the CM energy. R. Ayed et al. [31].

The Argand diagrams were then fit in several stages for each parametrization. First those partial waves with a substantial anti-clockwise arc on the Argand diagram were fit only one resonance. A second fit was then made with additional resonances allowed in those partial waves for which the «background» after the first fit was strongly suggestive of another resonance. All «backgrounds» except for the $S31$ wave were then quite smooth. It is particularly impressive, as can be seen in Fig. 11 for the $I = {}^1/_2$ waves, that the «background» speeds are very small and quite constant compared to the speeds for the total amplitude including resonance contributions. This is especially clear for the $D15$ and $F15$ waves for which the «backgrounds» are small and well behaved.

Figs. 12—13 show the fits resulting from the two parametrizations while using variable widths for the resonances in both cases. The phase shift and elasticity are plotted separately as a function of energy for each partial wave in Fig. 12 for the

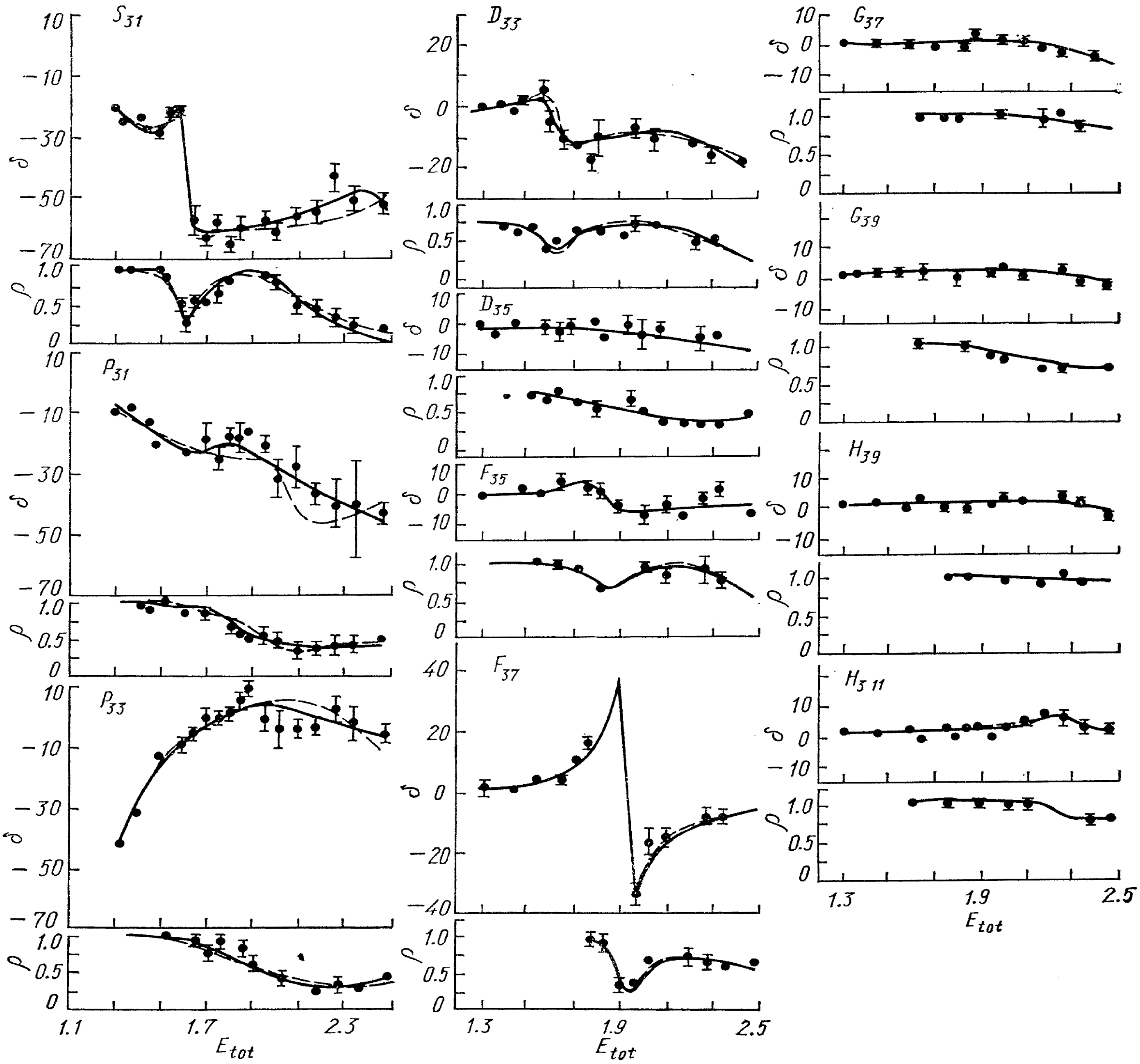

Fig. 12. Phase shifts (δ) and elasticities (ρ) for the $I = {}^3/_2$ isotopic spin states. The solid lines refer to parametrization 1 and the dashed lines to parametrization 2. The error bars give the «experimental phase shifts». R. Ayed et al. [31].

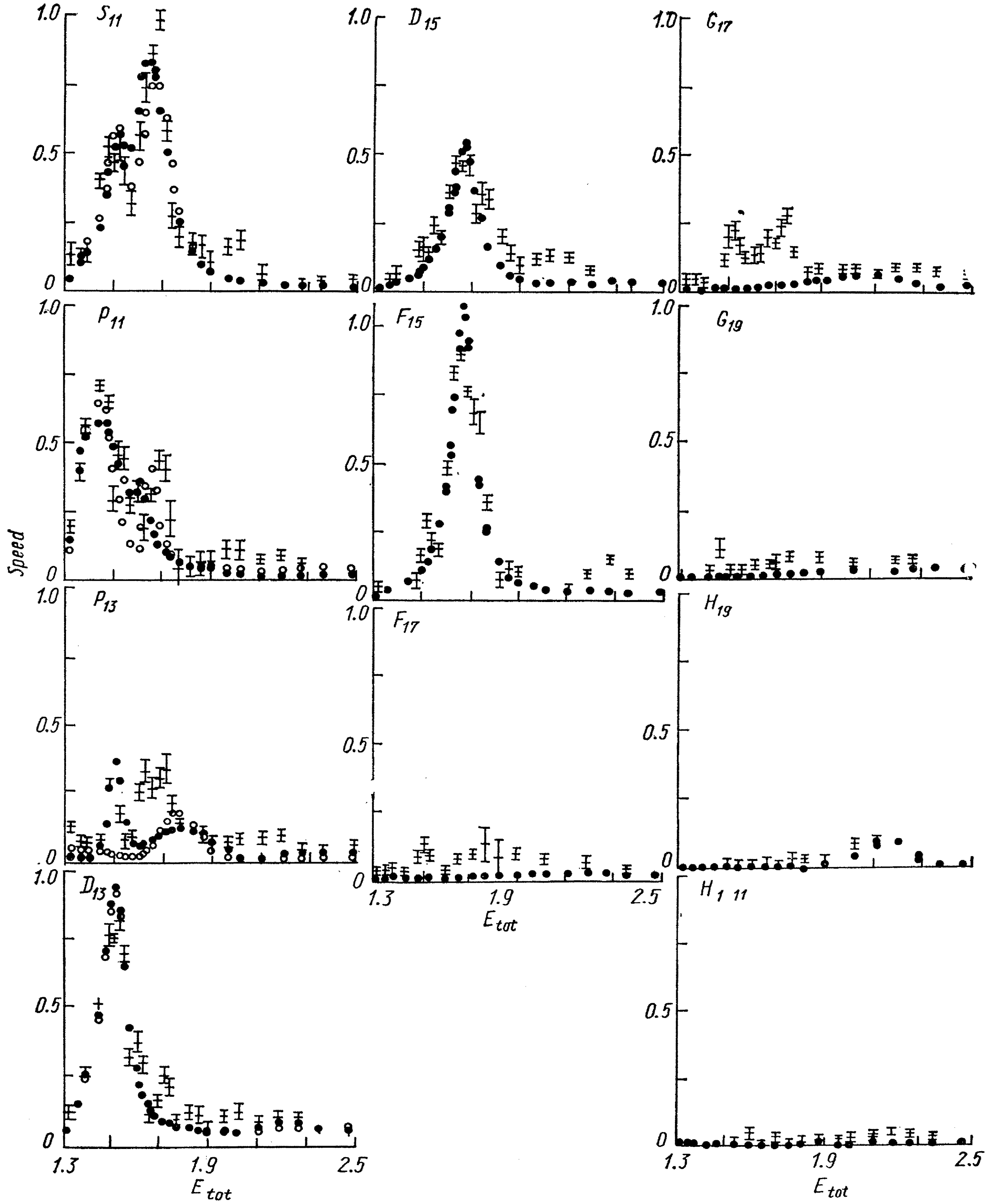

Fig. 13. Partial wave amplitude speeds for the isotopic spin $I = {}^1/_2$ waves. The error bars give the «experimental speeds» while the solid and open points correspond to the fitted amplitudes using parametrizations 1 and 2 respectively. R. Ayed et al. [31].

$I = {}^3/_2$ waves while Fig. 13 exhibits the speeds for the $I = {}^1/_2$ waves. The fits in general agree very well with the data except for possibly significant structures in the data in the $P31$ (1.6 *GeV*), $P33$ (1.7 *GeV*), and $P13$ (1.5 *GeV*) waves. The validity of the overall fit was checked by redoing the fit at each energy using the «smoothed» values as starting points. The observation that the new fit values did not differ significantly from the «smoothed» values helps to confirm the validity of the fit.

Table II

Nucleon Resonances
N^* Resonances — $I = 1/2$

	Particle Data Group [7]				Saclay [31]		
Name	J^P	Mass	Width	Status	Mass	Width	Status
* $P11$ (1470)	$1/2^+$	1470 ± 35	300 ± 100	OK	1470	190	OK
* $D13$ (1520)	$3/2^-$	1520 ± 20	125 ± 25	OK	1520	130	OK
* $S11$ (1535)	$1/2^-$	1550 ± 50	100 ± 50	OK	1550	110	OK
* $D15$ (1670)	$5/2^-$	1670 ± 15	140 ± 35	OK	1680	160	OK
* $F15$ (1688)	$5/2^+$	1685 ± 10	140 ± 40	OK	1690	110	OK
$D13$ (1700)	$3/2^-$			??		Omit	
* $S11$ (1700)	$1/2^-$	1710 ± 50	250 ± 150	OK	1680	170	OK
$P11$ (1780)	$1/2^+$	1805 ± 55	360 ± 90	?	1630	55	?
$P13$ (1860)	$3/2^+$	1870 ± 30	380 ± 70	?	{ 1896 1500	490 50	? ?
$F17$ (1990)	$7/2^+$	$1990\pm?$	$230\pm?$	?		Omit	
$D13$ (2040)	$3/2^-$	$2040\pm?$	$260\pm?$	?		Omit	
* $G17$ (2190)	$7/2^-$	2130 ± 130	$300\pm?$	OK	2200	400	
* $H19$ (2220)	$9/2^+$	—	—	—	2220	240	OK
		3245		??			OK
		3690		??			
		3755		???			
Δ Resonances — $I = 3/2$							
* $P33$ (1236)	$3/2^+$	1236 ± 0.6	120 ± 2	OK	1230 ± 0.6	114 ± 3	$(\Delta^{++})^8$
* $S31$ (1650)	$1/2^-$	1660 ± 40	190 ± 60	OK	1640	150	OK
* $D33$ (1670)	$3/2^-$	1670 ± 20	240 ± 60	OK	1640	160	
$P33$ (1690)	$3/2^+$			??	1800	600	??
$F35$ (1890)	$5/2^+$	1875 ± 35	260 ± 130	?	1840	190	?
$P31$ (1910)	$1/2^+$	1885 ± 50	330 ± 100	?	{ 1780 2070	310 310	??
* $F37$ (1950)	$7/2^+$	1940 ± 40	180 ± 40	OK	1930	190	OK
$D35$ (1960)	$5/2^-$			??		Omit	
$P33$ (2160)	$3/2^+$			??		Omit	
* $H311$ (2420)	$11/2^+$	$2420\pm?$	$310\pm?$	OK	2320	300	OK
		2850	400				
		3230	440				

* Definite and well measured.

The adequacy of the fit was tested by averaging the quantity $G_i = \chi_i^2/N_i - 1$, where N_i is the number of degrees of freedom (and χ_i^2 is the chisquared value) at the i-th energy. While zero is expected, the fit gave $G = 0.67 \pm 0.5$.

Table II summarizes the results of this analysis [31] and lists the major known properties of all nucleon resonances as listed by the Particle Data Group [7] for comparison. The mass and width errors listed in the table are not to be interpreted in the sense of standard deviations, but indicate the range obtained by various analyses due to differences in procedures and models while analyzing essentially the same data. While not well defined, these error indicators give probably the best available simple indication of the reliability and accuracy of the fits. An asterisk is used to denote those states whose existence is clear and whose parameters are relatively well determined.

The most striking result of this phase shift analysis [31] is the discovery with good evidence of two new resonances — *H*19 (2220) and *H*3, 11 (2315). These are the most massive nucleon resonances yet discovered with the elastic phase shift technique and are consistent with being Regge recurrences of the *F*15 (1690) and *F*37 (1950) respectively. They make adequate fits to a straight line on a Chew — Frautschi plot. The *H*3, 11 (2315) is somewhat low, but this mass is close to the top of the energy region treated in the fit and so is less constrained by the requirements of continuity.

In general this analysis confirms the results of previous phase shift analyses, although a number of questionable candidates — *D*35 (1960), *P*33 (2160), *D*13 (1700), *F*17 (1990), and *D*13 (2040) — are not observed, and a few others are found with weak evidence or with parameters violently different from earlier analyses. Particularly noteworthy are:

1. The *P*31 (1910) which is found here with poor evidence at 1780 *MeV* in parametrization 1 (Resonance + Background) and at 2070 *MeV* in parametrization 2 (Resonance * Background).
2. The *P*11 (1785) which is here found with a mass of 1630 *MeV* and a width of 55 *MeV*.
3. The *P*13 (1860) for which poor candidates are observed at 1500 *MeV* and 1900 *MeV*.
4. Other known resonances which are observed but classified as «poor» include the *P*33 (1690) — observed at 1800 *MeV*, and the *F*35 (1890).
5. Resonances not required by this analysis but for which some poor evidence previously existed include the *D*35 (1960), the *P*33 (2160), the *D*13 (1700), the *F*17 (1990), and the *D*13 (2040). Some evidence for the *D*13 (1700) is visible from the speed graph for the *D*13 wave in Fig. 13.

These examples indicate some of the limitations and inaccuracies of the elastic phase shift technique. Of greater importance is the fact that the thirteen resonances marked with asterisks in Table II are not controversial and have rather small errors on their parameters. This result is independent of detailed assumptions on the formalism used to represent background and resonances and the procedure used.

More precise data — some of which are already available — will clarify the situation further and there is hope that similar data at higher energies will permit an extension of the mass region, although the difficulties and complications above 3 or 4 *GeV* are difficult to foresee at the present time. Certainly the increase in the number of parameters as the number of important angular momentum waves increase and probable increases in inelasticities will complicate the analysis considerably.

It is quite likely that to push this type of analysis to higher energies more detailed models will be necessary. Such a model has been proposed by Wrighton, Ross, and Leith [32]. The validity and usefulness of such models are not entirely clear now, but the good agreement with experiment of this simple model is encouraging and may lead to deeper understanding.

This model [32] makes a direct fit to 56 differential cross sections and 49 polarization measurements in the invariant mass region 1.36—1.93 *GeV* using a sum of resonant plus diffractive background contributions to the *T* matrix. The resonant term used is a Breit — Wigner with energy dependent width and appropriate barrier penetration factors. The diffraction amplitude used to describe background is an exponential with constant slope in momentum transfer and a magnitude set by a constant fraction of the smoothed zero degree cross section obtained using

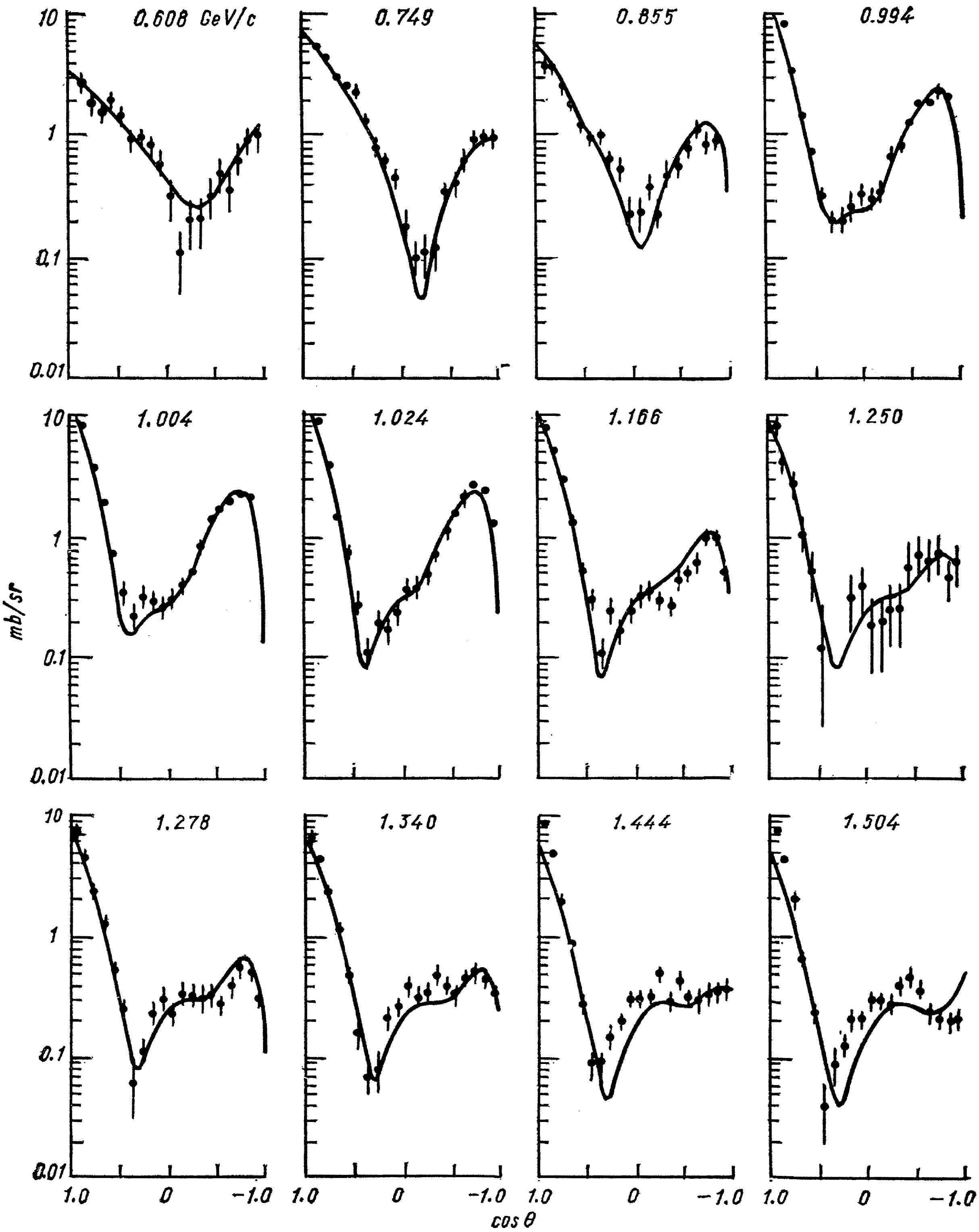

Fig. 14. π^- p differential cross sections from 1520 to 1995 *MeV* center of mass energy. The solid line is the fit of the model of G. C. Wrighton et al. [32].

the optical theorem. The phase between resonant and diffraction amplitudes is taken to be zero.

The resulting fit illustrated in Fig. 14 has a χ^2 of 9352 for 2126 degrees of freedom, but follows the main features of the data in spite of occasional discrepancies such as missing the diffractive peak at the higher energies. The fitted resonance parameters are compatible with the accepted values and in particular, the *F*11 (1785) is strongly supported at a mass of 1703 *MeV*.

Another technique designed to extend phase shift analyses to higher energies called «Phase Band Analysis» has been proposed by Moravcsik [33]. This technique divides the partial waves into two sets — angular momentum states $l = 0$ to l_0, which are treated collectively by, for example, writing the elasticity and phase shift as polynomials in l — and angular momentum states $l = l_0 + 1$ to $l_{\max}$ which are treated individually in the normal way. The advantage of the technique is a reduction in the number of free parameters ($4\,(2l_{\max} + 1)$ in a normal analysis), which become very large when many angular momentum states must be considered.

Table III

Analysis of $\pi N \to N\pi\pi$

Reaction	ECM	Events	Group	Ref.
$\pi^- p \to \{N^*\pi\} \to n\pi^+\pi^-$	1.36—1.45 (4)	2.3*K*	Leningrad	[35]
$\pi^+ p \to \{N^*\pi\} \to n\pi^+\pi^+,\ p\pi^+\pi^0$				
$\pi^- p \to \{N^*\pi\} \to n\pi^+\pi^-,\ p\pi^-\pi^0,\ n\pi^0\pi^0$	1.34—1.44 (4)	?	Leningrad	[36]
$\pi^- p \to \left\{ {N^*\pi \atop N\sigma} \right\} \to n\pi^+\pi^-,\ p\pi^-\pi^0$	1.34—1.40 (4)	7.8*K*	Oxford	[37]
$\pi^+ p \to \{N^*\pi\} \to p\pi^+\pi^0$ $\pi^- p \to \{N\sigma\} \to p\pi^-\pi^0,\ n\pi^+\pi^-$ $\pi^+ n \to \{N\rho\} \to p\pi^+\pi^-$	1.68—1.97 (4) 1.39—1.53 (4)	19.4*K* ~8*K*	Saclay	[38] [39]
$\pi^- p \to \{\Delta^-\pi^+\} \to n\pi^+\pi^-$	1.64—1.70 (11)	52*K*	SLAC—UCRL	[40]
$\pi^+ p \to \left\{ {\Delta^{++} \atop p\rho^+\pi^0} \right\} \to p\pi^+\pi^0$	1.85—2.09 (6)	42*K*	Riverside—UCRL New Hampshire	[41]

The technique may be applicable at energies high enough so the low partial waves are mainly absorbed and hopefully uncoupled. The method was tested at 2.5 and 2.75 *GeV/c* and gives results in agreement with standard techniques [34]. The solutions were tested for stability by taking larger and smaller collective bands with encouraging results. The work is being continued in an attempt to fit all partial waves by iterating while decreasing the collective band and fixing the higher waves until all waves are determined in detail. A fairer test of the technique requires complete data at considerably higher energies where the number of parameters would normally be excessive.

B. The Isobar Model. The reaction $\pi N \to N\pi\pi$ is the major inelastic channel in the resonance region and, in principle, can produce very useful information to supplement the elastic phase shift analyses. In particular, resonances with very small elastic branching ratios produce small circles which are difficult to reliably isolate on Argand diagrams (smoothing techniques tend to erase them), but could be readily observed if they had a large branching ratio to $N\pi\pi$. Difficulties arise because of the three body final state which the isobar model assumes to be a quasi two body final state consisting of a resonance which decays into two particles plus the third particle. This is certainly an incomplete description and a

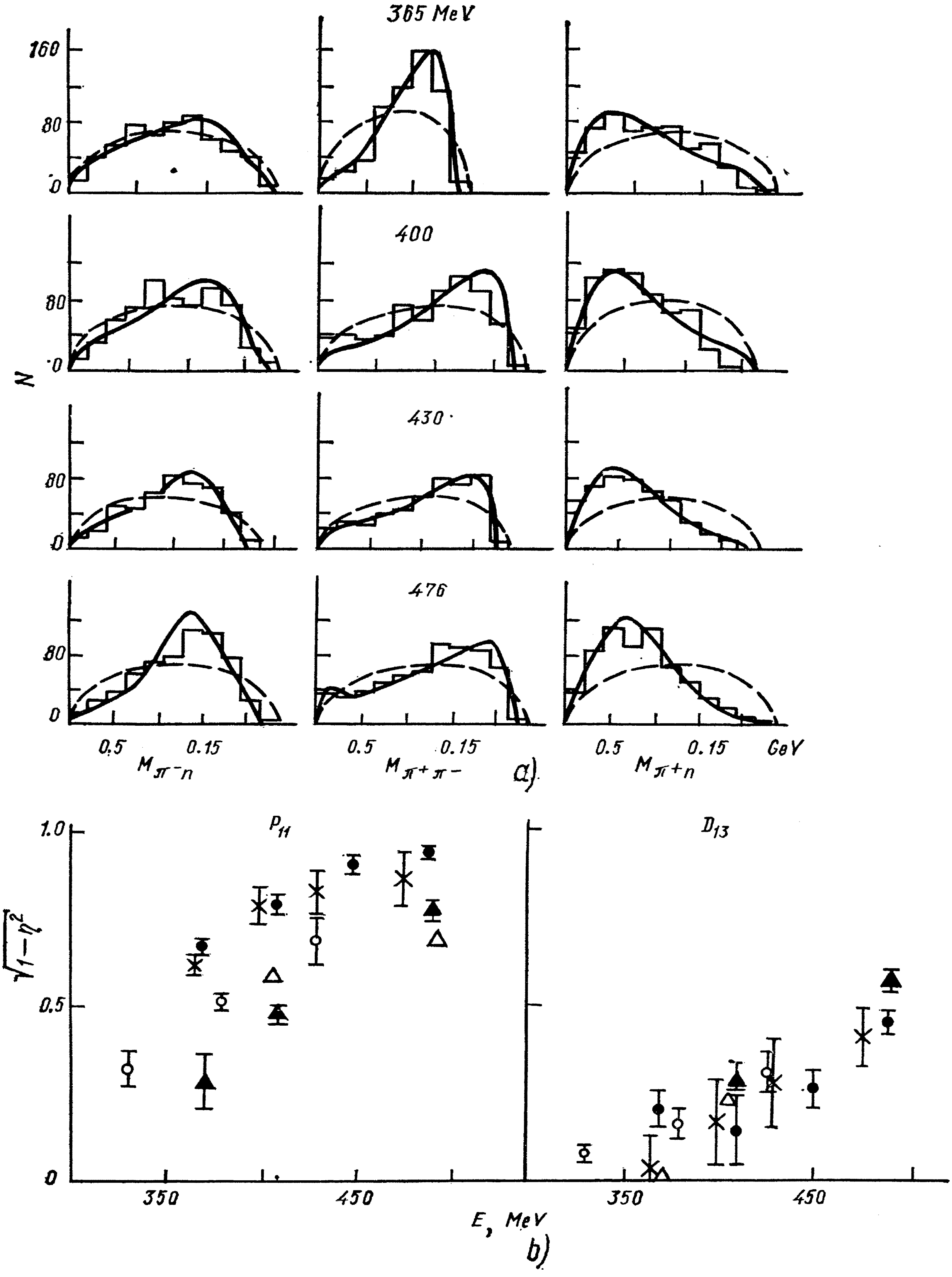

Fig. 15. (*a*) Invariant mass spectra from the reaction $\pi^- p \to n\pi^+\pi^-$. The dotted curves show phase space and the solid curves exhibit the fit of the model. (*b*) The elasticities calculated from the model (stars) compared to the phase shift fits of CERN [21] (closed circles), Saclay [28] (open circles), and the isobar model fits of Saclay [45] (open triangles), Oxford [37] (closed triangles). M. M. Makarov et al. [35].

coherent mixture of all possible resonances plus background is required to describe the reaction completely. Starts have been made in this direction, but more data and detailed fits are required.

Table III summarizes the contributions in this area. In general, reasonable fits have been made to the data and the elastic branching ratios found from the fits are in fair agreement with the results of elastic phase shift analyses.

Makarov et al. [35] have carried out a relativistic partial wave analysis [42] of the reaction $\pi^- p \to n\pi^+\pi^-$ using four diagrams, but ignoring $\pi\pi$ interactions. Using the nomenclature L_i, L_f, $2J$, where L_i, L_f are the orbital angular momenta of the initial and (quasi two body) final states, and J is the total angular momentum, Δ (1236) production was assumed in the $DS3$, $DD3$ and $PP1$ states, and background in the $PS1$ state. Fitting the model at each energy separately to the pion angular distributions, a reasonable fit to the data was obtained as shown in Fig. 15*a*. Evidence is obtained for the branching ratio of the $P11$ (1470) into $\Delta\pi$ to be about 50%, but the maximum energy of this experiment is below the central mass of the $P11$ (1470). The elasticity parameter has also been determined for the $P11$ and $D13$ incident waves and agrees rather well with the elastic phase shift data as shown in Fig. 15*b*.

Kravtsov [36] has analyzed both $\pi^+ p$ and $\pi^- p$ going into five different channels assuming all events proceed through the $N^*\pi$ channel where N^* is either the Δ (1236) proceeding through the $DS3$ or $PP1$ waves or a N^* ($^1/_2$, $^1/_2$) treated in the scattering length approximation. $\pi\pi$ interactions are ignored, but interference effects are included leading to an 11 parameter fit at each four energies. Again, reasonable agreement with the data was obtained and agreement with the elastic phase shift analyses was obtained — the agreement with the CERN [21] analysis is considerably better than that with Saclay [28] or Schegelsky [43], as shown in Fig. 16.

A detailed application of the isobar model to both $\pi^+ p$ [38] and $\pi^- p$ [39] induced reactions was carried out by a group at Saclay on a total sample of about 27*K* events, most of which were measured at other laboratories. This analysis, which is similar to that of Saxon, Mulvey, and Chinowsky [37] on $\pi^- p$ reactions at a slightly lower energy, used N ($\pi\pi$) intermediate states as well as the ($N\pi$) π state employed by Makarov et al. [35] and Kravtsov [36]. It is perhaps not surprising that at low energies, where the s wave is dominant, the ($N\pi$) π and N ($\pi\pi$) formalisms give similar results. Above 1500 *MeV*, however, it is clear that p wave ($\pi\pi$) interactions must be included [37, 38].

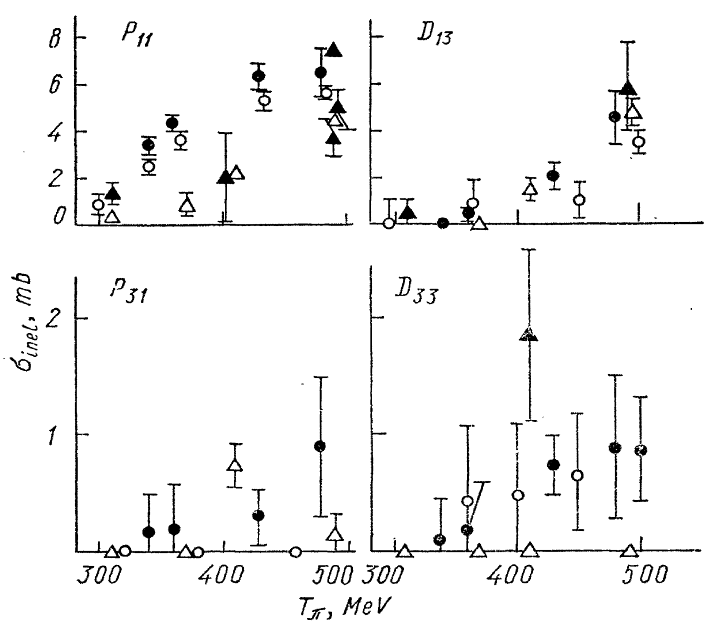

Fig. 16. Partial wave cross sections for $\pi N \to N\pi\pi$ as obtained from the isobar model fit of A. V. Kravtsov [36] compared to the results of the elastic phase shift analyses of Saclay [28] (open triangles), CERN [21] (open circles), and Schegelsky [43] (closed triangles).

The $\pi^- p \to p\pi^-\pi^0$, $n\pi^+\pi^-$ reactions were described by the Saclay group [39] as a coherent superposition of the $\pi\Delta$ (1236), $N\sigma$, and $N\rho$ intermediate states. The σ is not considered to be necessarily a real resonance, but a useful formalism to describe the $\pi\pi$ interaction in an $I = J = 0$ state as given

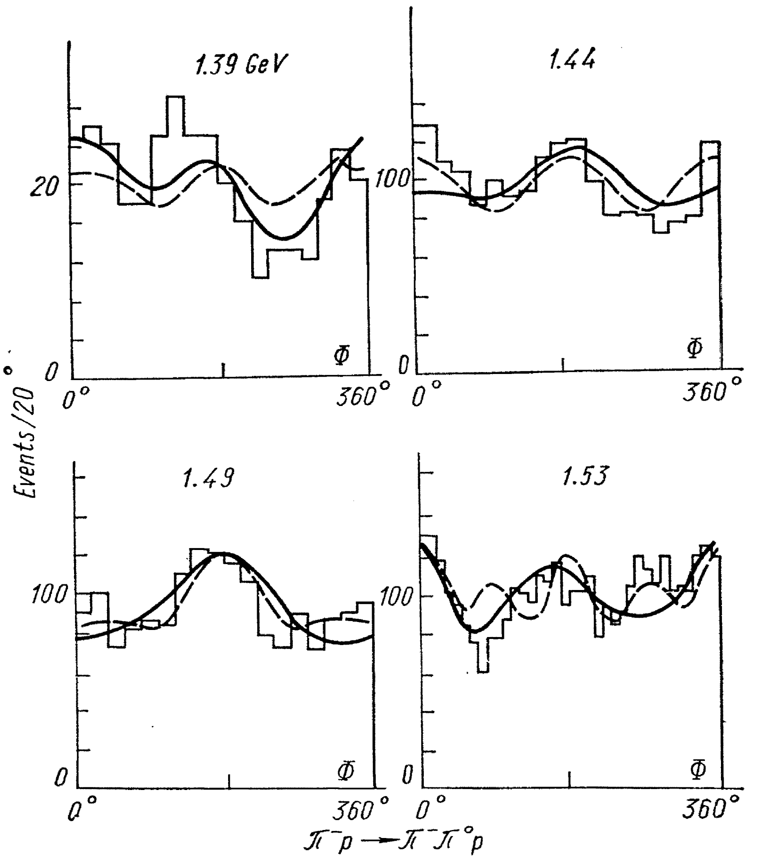

Fig. 17. Distribution of the azimuth angle of the incident π in a frame determined by the final particles. The solid lines indicate the fit of the model including the $N\pi$ intermediate state. Nguyen Thuc Diem et al. [39].

by $\pi\pi$ phase shifts [44]. Its mass was taken as 746 MeV and its width as either 200 or 400 MeV without noticeable differences in the fit, although lower masses were excluded by previous fits [45]. The partial waves used were $\pi\Delta$ ($PP11$, $SD11$, $DS13$, $PP13$, $DD13$, $SD31$, $DS33$, and $DD33$), $N\sigma$ ($PS11$, $SP11$, $DP13$), and $N\rho$ ($SS11$, $PP11$, $DS13$). The nomenclature here is L_i, L_f, $2I$, $2J$, where I is the total isotopic spin. In general, two couplings are possible for the $N\rho$ state in a given partial wave. In the $PP11$ state where this is possible, it was found that they gave equivalent results and only the $(N\rho)$ state with spin $^1/_2$ was kept. One overall phase is arbitrary and was fixed by giving the $DS13$ wave the phase of the elastic $D13$ amplitude. All parameters were then determined by fitting the data (including the reaction $\pi^+n \to p\pi^+\pi^-$ obtained from deuterium reactions) to this model.

A typical comparison with the data is shown in Fig. 17. The fit with the ρ included (solid line) is a clear improvement over the fit without the ρ (dotted line). The ρ channel decreased the total χ^2 by a factor of 2 to 3, giving 1.5 to 2 per degree of freedom.

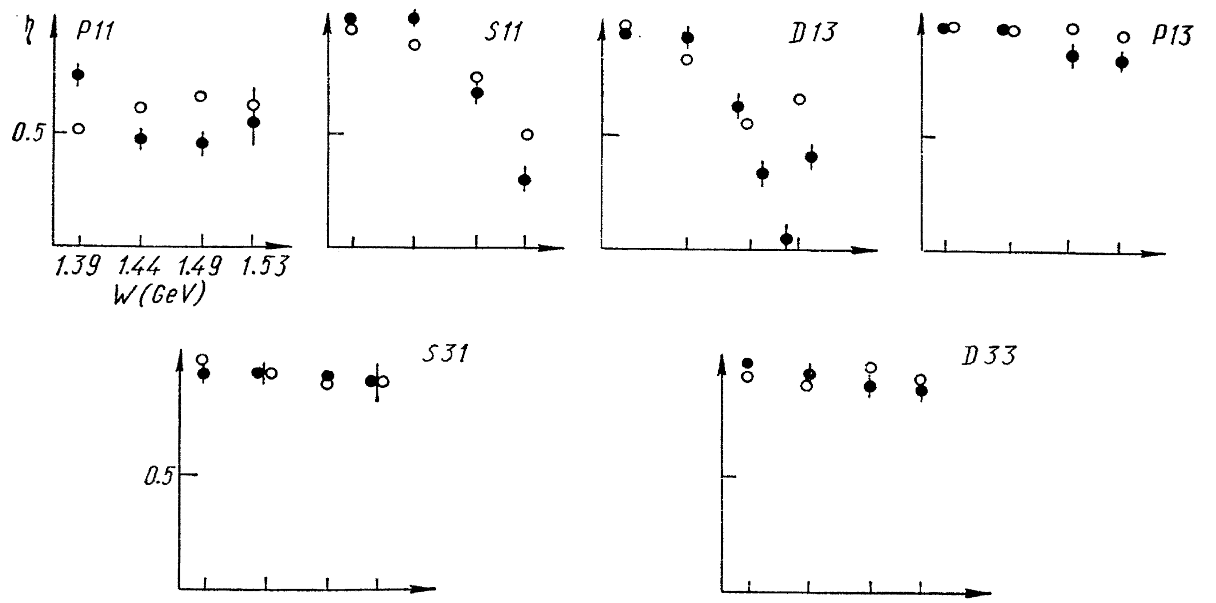

Fig. 18. Partial wave elasticity parameters as determined from isobar model fits [39] and the phase shift analysis of Saclay [18]. Nguyen Thuc Diem et al. [39].

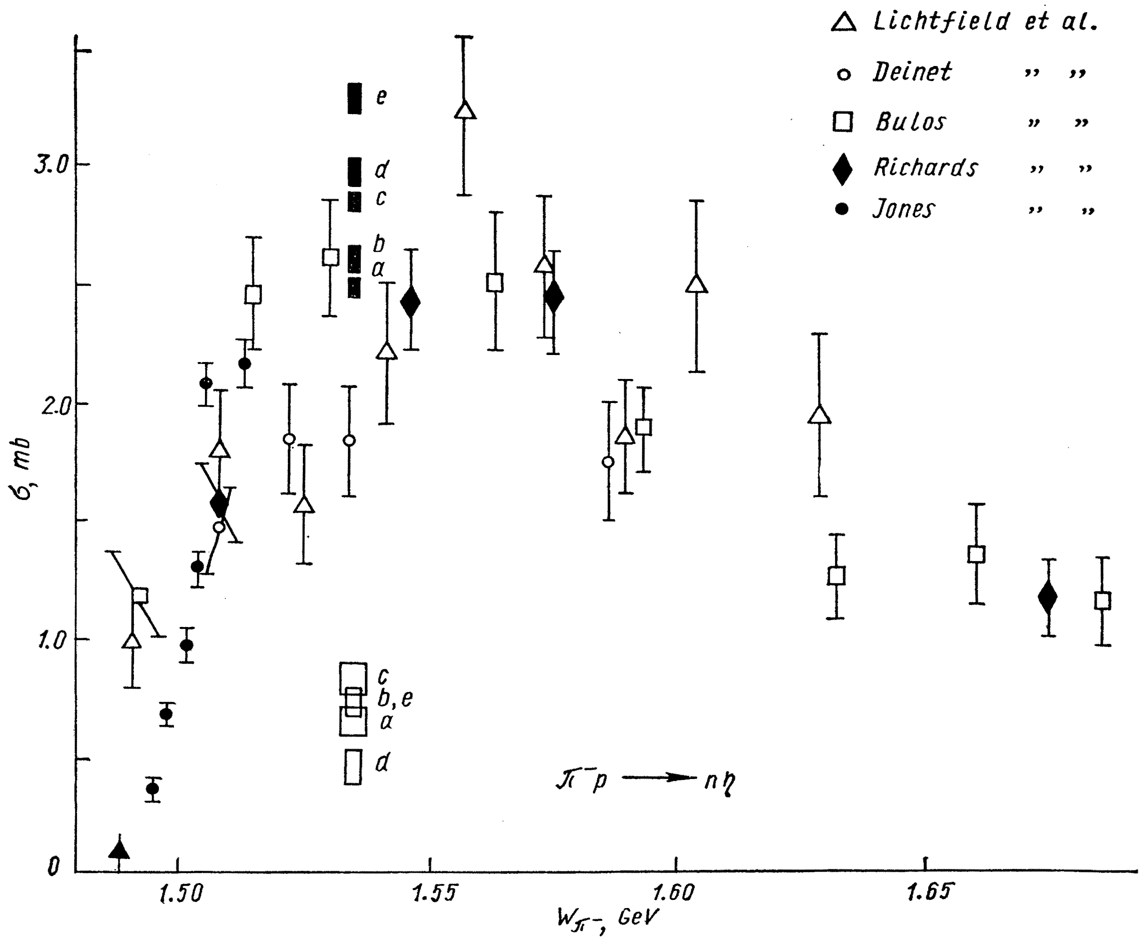

Fig. 19. Total cross section for $\pi^- p \rightarrow n\eta$. The solid boxes indicate the predictions of elastic phase shift analyses for the total cross section while the open boxes denote the contributions due to the $S11$ partial wave. Nguyen Thuc Diem et al. [39].

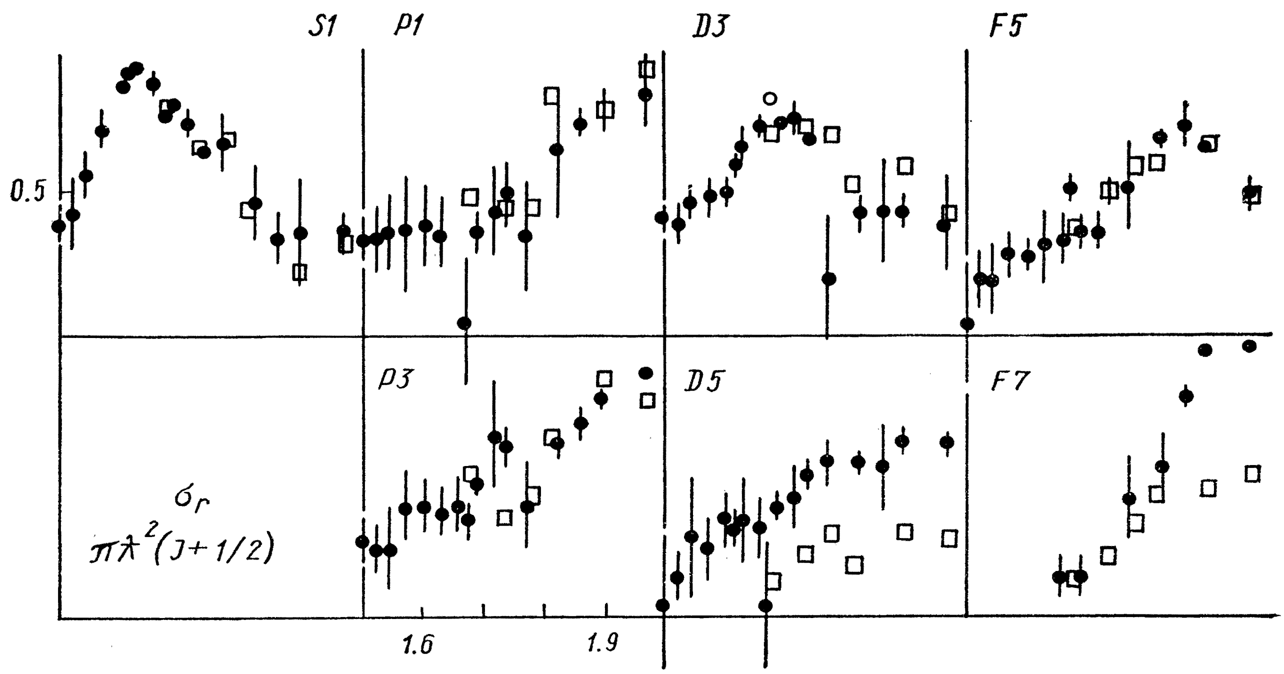

Fig. 20. Comparison between elasticity parameter obtained from an isobar model fit [38] and an elastic phase shift analysis [18]. P. Chavanon et al. [38].

Of particular interest for production experiments is the results that the $P11$ wave decay into $\pi\Delta$ is comparable to its decay into $N\pi\pi$. This branching ratio is extremely difficult to measure in production experiments as will be discussed and, of course, is not observable in elastic phase shift analyses.

A comparison with the elasticities from elastic phase shift analyses is possible since the cross sections for inelastic channels other than $N\pi\pi$ is small at these energies. Good agreement is obtained as shown in Fig. 18. At the higher energies, this experiment yields larger elasticities (smaller inelastic cross sections) as would be expected from the increase of other inelastic channels as the energy increases.

The data are consistent with all the «missing inelasticity» at 1.53 GeV (2.2 mb) being in the $n\eta$ channel. The total cross section obtained for this reaction is compatible with other measurements as shown on Fig. 19. However, the dominant wave responsible is $D13$, and $S11$ contributes only 10—16%, a result in complete disagreement with the K matrix analysis of Davies and Moorhouse [22].

The analysis of $\pi^+p \rightarrow p\pi^+\pi^0$ [38] was carried out in a similar way, except that higher angular momentum states were included due to the higher energies involved, and the $N\sigma$ channel was not included. Instead 10 partial waves (up to $FF7$) were used for the $\pi\Delta$ channel and 4 for each ($N\rho$) spin state. This gave 18 partial waves with 35 parameters (the arbitrary phase was set by taking the phase of the $FF7$ wave to be that of the $F37$ elastic amplitude).

The agreement with the elastic phase shift analysis [18] is good for all waves except $D35$ and $F37$ (see Fig. 20), which may be corrected by other channels such as $\pi^+p \rightarrow \Sigma^+K^+$. Some evidence is seen for the $D33$ (1670) decaying into both $\Delta\pi$ and $N\rho$ and the $P33$ (1690) is observed, if at all, at a mass of 1.8 GeV or higher.

The general agreement of the fit with the data is reasonably good except at the highest energies as would be expected. It may be that peripheral production mechanisms are beginning to be important, and such effects will be included in the next series of fits by this group [38, 39].

There is evidence that the isobar model is currently a phenomenology accurate to perhaps 10% [38, 39]. This is roughly indicated by the general quality of the fits at lower energies. It would clearly be valuable to improve this phenomenology and to obtain adequate statistics to check the phenomenology more carefully. In particular, at higher energies the

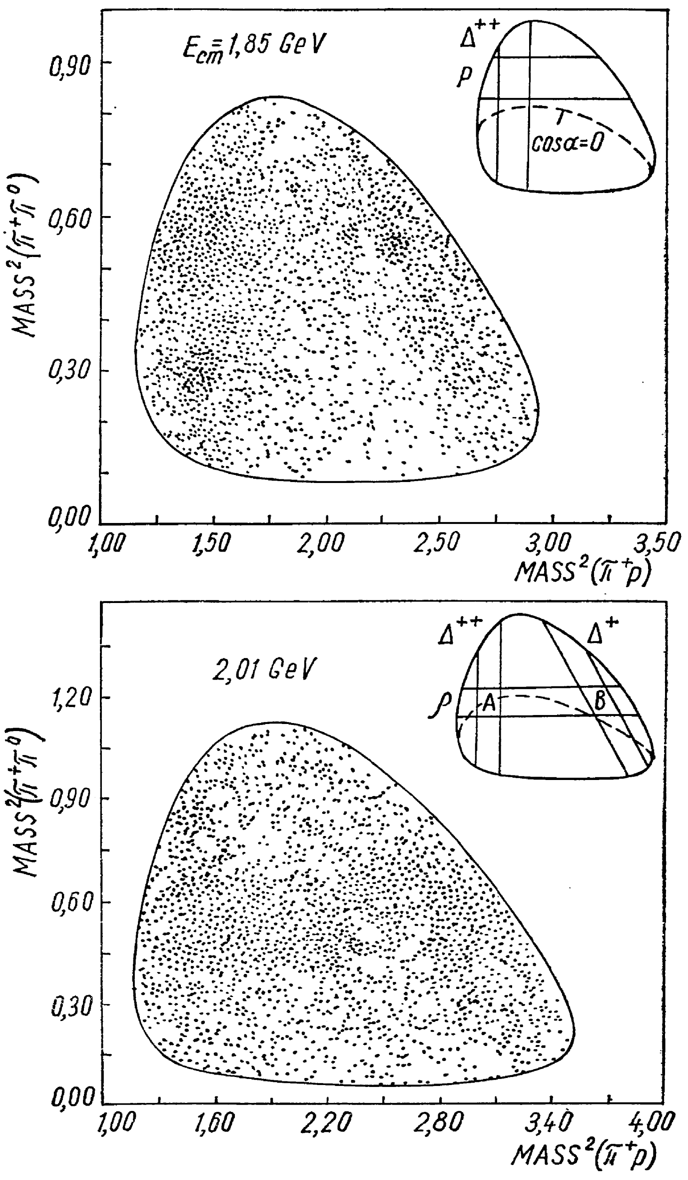

Fig. 21. Dalitz plots for $\pi^+p \rightarrow p\pi^+\pi^0$ at two energies to illustrate the overlap between Δ^{++} (1236) and ρ^+ bands. U. Mehtani et al. [41].

problems increase due to the importance of higher partial waves, more resonances and peripheral processes.

A Riverside — Berkeley — New Hampshire collaboration reported on a very large statistics study of the $\pi^+p \to \Delta^{++}$ (1236) π^0 channel [41]. 1.2 million pictures were analyzed at six momenta in the invariant mass region 1.85—2.09 *GeV* yielding 42*K* events in the channel $\pi^+p \to p\pi^+\pi^0$ which is dominated by the quasi two body channels $\Delta^{++}\pi^0$, $\Delta^+\pi^+$ and $p\rho^+$. The technique used to select out the Δ^{++} (1236) π^0 channel was to make cuts on the Dalitz plot. As shown in Fig. 21, this selection is not straightforward due to the overlap of the Δ^{++} (1236) and ρ^+ bands. To minimize this difficulty, only the lower half of the Δ^{++} (1236) band was taken at lower energies which gives half the angular region of the Δ^{++} (1236) decay in an unbiassed fashion. Note that M^2 ($\pi^+\pi^0$) is linear in cos α for fixed M ($p\pi^+$), where α is the CM decay angle of the Δ^{++} (1236). At higher energies, where the ρ^+ band crosses the middle of the Δ^{++} (1236) band (Fig. 21*b*), the mass conjugation technique of Eberhard and Pripstein [46] was used. This assumes the quasi two body amplitudes are incoherent and that the Δ^{++} (1236) π^0 and Δ^+ (1236) π^+ amplitudes are identical.

Both *s* channel resonance effects (seen in the rapid variations of the cross section) and *t* channel ρ-exchange effects (dips at $t_{\min}$ and $t = -0.5$ $(GeV/c)^2$) are clearly visible in the data (Fig. 22). A fit was made using four resonances in this energy region — *F*35 (1890), *P*31 (1910), *F*37 (1950) and *D*35 (1960) — as well as four adjoining resonances whose parameters were held fixed at their reported values [7]. The fit, which is shown by the broken line in Figure 22, has a chisquared of 274 with 103 degrees of freedom (χ^2 = 274/103), with the worst disagreement at

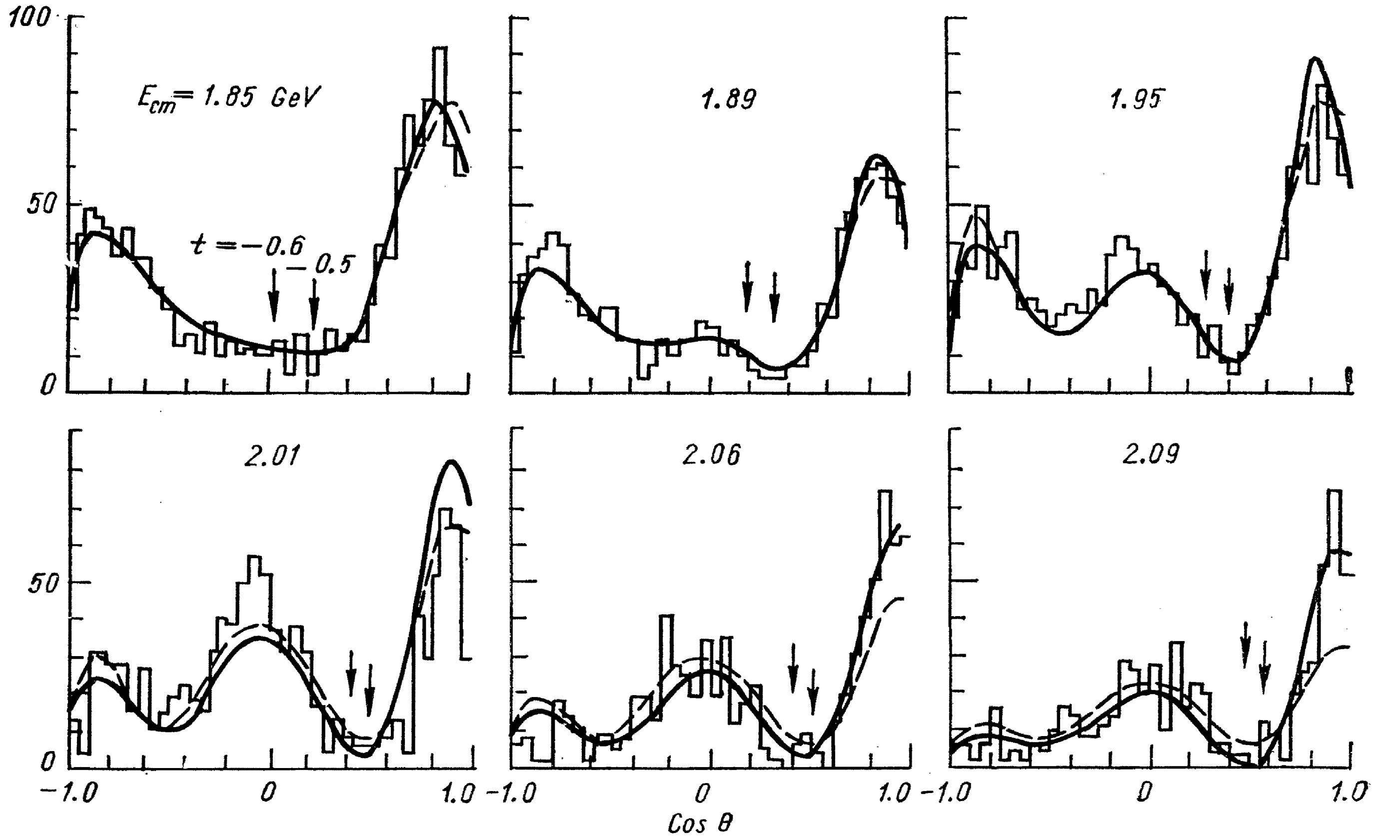

Fig. 22. Distributions in the center of mass angle between the π^+ and π^0 in the reaction $\pi^+p \to$ $\to p\pi^+\pi^0$. The broken line is the fit for *s*-channel resonances while the continuous line is the fit for a coherent sum of *s*-channel resonances and ρ exchange. U. Mehtani et al. [41].

the higher energies. A second fit was then made with a coherent sum of s-channel resonances as described above and a completely determined Regge ρ exchange amplitude. This improved the chisquared to 221/103 and the fit is shown by the continuous line in Fig. 22. This fit, of course, contains the danger of double counting in that the s-channel resonances may already be contained in the t-channel amplitude. To check this, the s-channel partial wave amplitudes were projected out of the t-channel amplitude. No clear resonance—like amplitudes were observed. The resonance parameters obtained in either fit are not in disagreement with the results of elastic phase shift analyses.

In studying the $p\rho^+$ channel [47], the same group has found no evidence for decays of nucleon resonances into the ρN channel.

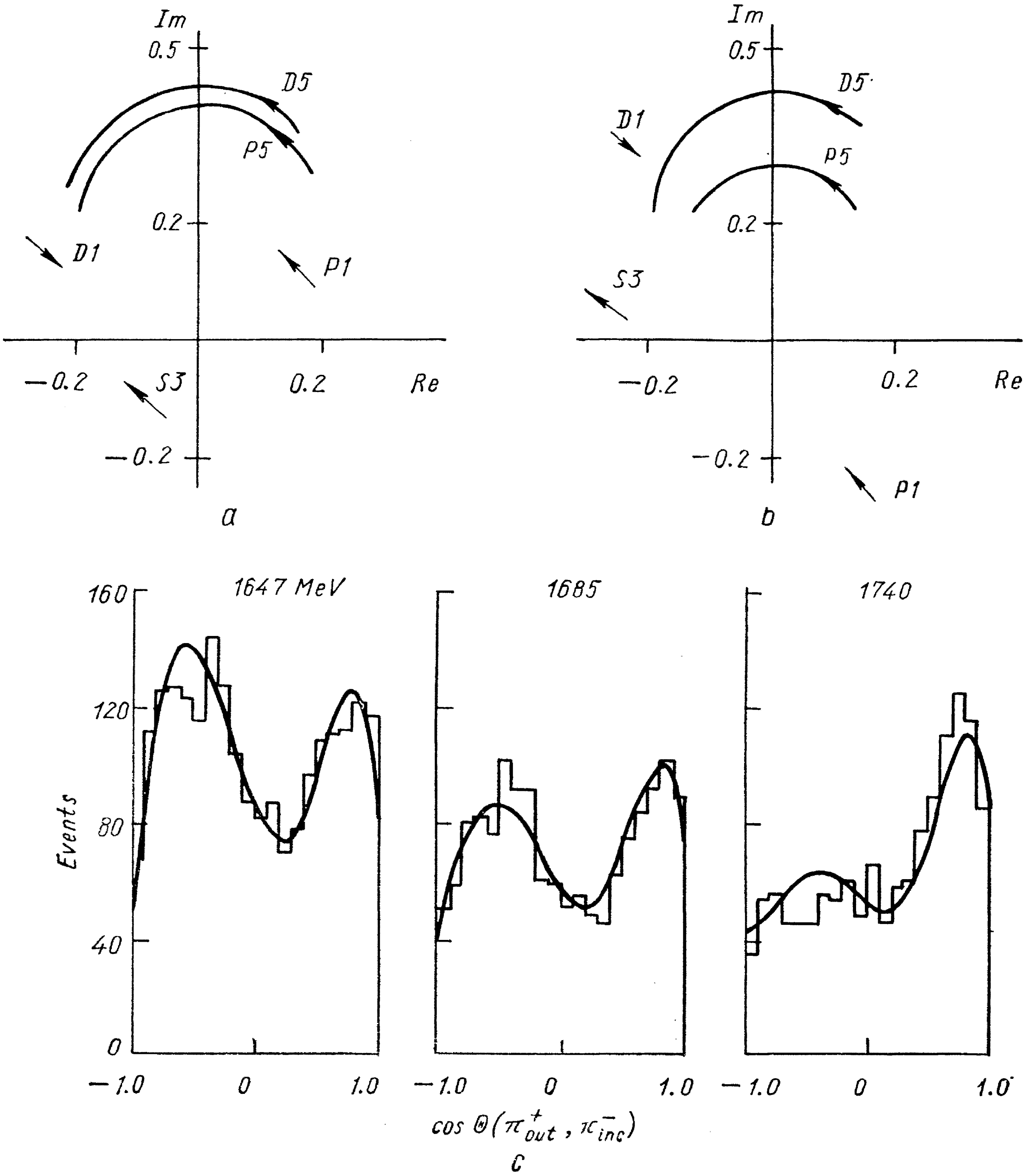

Fig. 23. Variation of partial wave amplitudes for the reaction $\pi^- p \to \Delta^-$ (1236)π^+ when fitting (*a*) production angular distributions only, (*b*) both production and decay distributions. (*c*) typical fits to the production angular distribution. A. D. Brody et al. [40].

An analysis of the reaction $\pi^- p \rightarrow \Delta^-(1236)\,\pi^+$ was used to measure the $\Delta\pi$ branching ratios of the $D15$ (1670) and $F15$ (1688) resonances to be 0.44 ± 0.08 and 0.26 ± 0.06 respectively [40]. The quasi two body channel was selected from $\pi^- p \rightarrow n\pi^+\pi^-$ by selecting the $n\pi^-$ mass to lie in the region $1140 < M(n\pi^-) < 1320$ MeV. A partial wave analysis was carried out including the $P5$ and $D5$ waves to describe the resonances and $S3$, $P1$, $D1$, and $F7$ waves to describe the background. The nomenclature is L, $2J$, where L is the $\pi\Delta$ orbital angular momentum and J is the total angular momentum. Resonances were parametrized by nonrelativistic Breit — Wigner amplitudes with mass dependent widths and backgrounds by $T = (a + bq) + i(c + dq)$ where q is the $\Delta\pi$ CM momentum. The general quality of the fits and partial wave amplitudes are shown in Fig. 23.

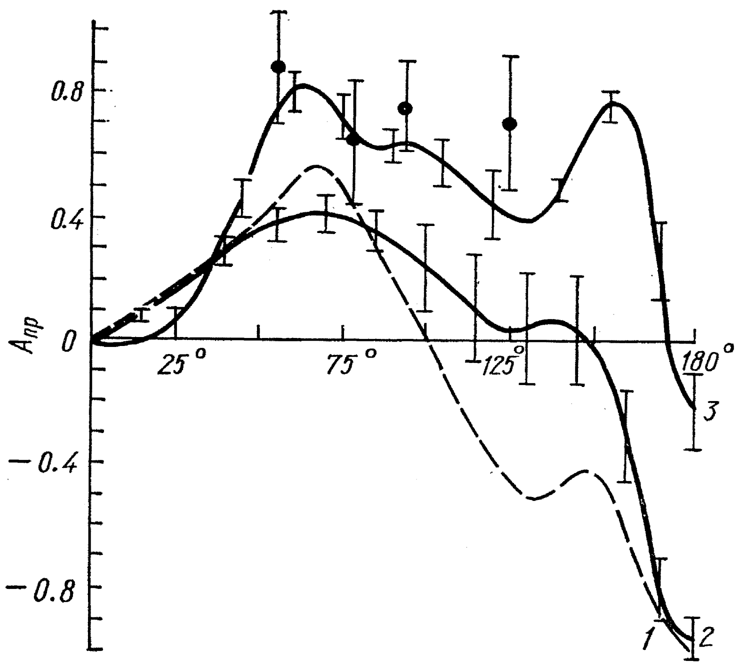

Fig. 24. The Wolfenstein parameter A_{np} as measured at 605 MeV [49] (solid circles) compared with the phase shift predictions of Pazman et al. [51]. S. I. Bilenkaya et al. [49].

Measurements of the Depolarization D_{pn} [48] and of the Wolfenstein parameter A [49] in elastic pn scattering at 605 MeV were also reported. The purpose of these experiments was to distinguish between two existing sets of nucleon—nucleon phase shifts in the energy range 600—650 MeV [50]. As shown in Fig. 24, the A_{pn} measurements reject solution II of Pazman et al. [51] and agree well with solution III. This extends the region in which the phase shifts are uniquely known from 400 to 650 MeV, but depends on the assumptions used in the fit that $l > 5$ states are reasonably described by a one-pion exchange diagram and on assumptions on the meson production mechanism.

III. Production Experiments

A. N^* (1400—1700). Most of the contributions on the production of nucleon resonances were concerned with the $N\pi\pi$ state in the invariant mass region 1400—1700 MeV. The properties studied included the existence of the 1470 and 1700 MeV bumps, their mass and width values, the branching ratio of the N^* (1700) to Δ (1236) π, and attempts at angular momentum analysis.

As discussed earlier, the correlation between bumps in invariant mass distributions and resonance parameters derived from elastic phase shift analysis is not straightforward as σ_{inel} may peak at a considerably different mass than the central resonance mass due to the effects of background. Further, the background may differ among different production experiments and should be quite different from the background in formation experiments. The $F15$ (1690) and $D15$ (1670), which are presumably mainly responsible for the bump around 1700 MeV to be discussed, have considerably less background than the $P11$ (1470) in formation experiments and the 1700 bump is better behaved in production experiments but

Table IV

Production Experiments on the N* (1470) and N* (1700)

	N* (1470)				N* (1700)					
Reaction	Momen. GeV/c	Events	M	Γ	M	Γ	$\frac{\Delta\pi}{N\pi\pi}$	$\frac{\Lambda K}{N\pi\pi}$	Group	Ref.
$K^-p \to K^-p\pi^+\pi^-$	4.2	4.5K	—	—	1726±6	83±13	<10%	—	Nijmegen — Amsterdam	[52]
$\pi^+p \to p\pi^+\pi^+\pi^-$	5.0	7.0K	—	—	1710±10	66±26	<20%	<4%	Bonn et al.	[53]
$\pi^-p \to p\pi^+\pi^-\pi^-$	6.0	~8K	—	—	1730±15	130±30	~0	5±1%	BNL	[54]
$K^-p \to K^-p\pi^+\pi^-$	3.9, 4.6 7.3	13.9K 3.9K	1479±11 1466±15	110±26 130±30	1707±8 1720±10	65±20 75±20	<8%	4±1.5%	BNL	[55]
$K^+p \to K^+p\pi^+\pi^-$	10.0	7.1K	~1480	—	~1690	—	—	—	Birmingham — Glasgow — Oxford	[56]
$\pi^+p \to \pi^+p\pi^+\pi^-$	8.0	5.8K	1458±20	52±30	1702±20	50±30				
$K^-p \to K^-p\pi^+\pi^-$	10.1	6.9K	1474±15	61±20	1713±15	64±20	75	—	ABBCHLV	[57]
$\pi^-p \to \pi^-p\pi^+\pi^-$	16.2	4.0K	1472±15	57±20	1706±10	68±20	±15%			
$\pi^+p \to \pi^+p\pi^+\pi^-$	16.0	2.0K	—	—	—	—				
Combined Events			1467±10	72±15	1713±10	124±20				
$\pi^-p \to \pi^-p\pi^+\pi^-$	7.0 25.0	5.0K 2.1K	1510±10 1510±20	80±15 100±30	1690±10 1700±10	110±20 70±20	~0	>0	Wisconsin — Toronto	[58]
$\pi^+n \to p\pi^+\pi^-\pi^0$	7.0	1.9K	1460±10	120±30	1730±30	120±30				
$K^-n \to K^-p\pi^-$	12.6	0.3K	($p\pi^-$ Decay) M = 1442±30, Γ = 430±60				—	—	Johns Hopkins	[59]
$pp \to pp\pi^+\pi^-$ (π^0)	13.1	5.0K	~1470		~1690		N* (1750) → pω		Paris — CEN	[60]
$\pi^+p \to \pi^+p\pi^+\pi^-$	13.1	10.2K	—	—	1719±6	63±12	70 ±15%	<2.5%	Purdue	[61]
$\pi^\pm p \to \pi^\pm p\pi^+\pi^-$	16.0	3.6K	~1450		~1720		~100%	—	SLAC	[62]
$\pi^+p \to \pi^+p\pi^+\pi^-$	18.5	4.5K	1478±10	61±32	1732±7	34±14				
$\pi^-p \to \pi^-p\pi^+\pi^-$	18.5	4.6K	1426±8	58±8	1702±16	48±22	69		Notre Dame	[63]
$\pi^-p \to \pi^-p\pi^+\pi^-$	8.0	2.5K	1435±10	93±23	1696±9	56±21	±14%			
Combined		11.7K	1451±8	124±5	1707±8	78±15				
$np \to pp\pi^-$	2—10	0.8K	~1470	—	~1690	—	—	—	JINR	[64]
$\pi^-p \to \pi^-p\pi^+\pi^-$	6.0	0.5K	—	—	1730±18	55±15	—	—	Indiana	[65]
$\bar{p}p \to \bar{p}p\pi^+\pi^-$ (π^0)	5.7	6.0K	—	—	1695±9	70±20	~0	<2%	CERN	[66]
$pp \to pp\pi^+\pi^-$	22.0	1.2K	1443±15	100±15	1693±15	235±50	—	—	Iowa	[67]
$pp \to pp\pi^+\pi^-$	24.8	3.2K	1423±27	135±64	1688±23	116±48	~0	—	Rutgers — Columbia	[68]

this behavior is not a necessary consequence of the smaller background under the 1700 *MeV* resonances in production. Their somewhat smaller widths and increased distance above threshold do help to simplify this problem.

Table IV summarizes the contributions to this conference and previously published work relevant to the problems of the masses and widths as well as the Δ^{++} (1236) π^- and Λ^0 K branching ratios of the 1400 and 1700 bumps. The masses and widths show a remarkable consistency considering the variety of production reactions and energies. That the consistency is not perfect is well illustrated by Fig. 25 which shows the combined $p\pi\pi$ mass distribution from reactions of the type $mp \to mp\pi^+\pi^-$ including 8 *GeV/c* π^-p [63], 13.1 *GeV/c* π^+p [61], 16 *GeV/c* $\pi^\pm p$ [62] and 18. 5 *GeV/c* $\pi^\pm p$ [63]. The 1700 *MeV* bump remains striking as in the individual plots, but the 1470 bump visible in the individual plots becomes a shoulder. This could be due to different backgrounds in the various reactions, but the ABBCHLV collaboration [57] after combining in a similar way π^+p at 8 *GeV/c*, K^-p at 10 *GeV/c*, and $\pi^\pm p$ at 16 *GeV/c* with similar total statistics see a definite bump at 1450 *MeV* with a valley of almost 100 events/50 *MeV* separating it from the 1700 *MeV* bump.

The branching ratio into ΛK, while certainly not totally consistent, does not disagree by more than a few standard deviations. The evidence for its existence at around the 5% level now seems to be quite convincing [54, 55]. However, the disagreement on the Δ (1236) π branching ratio of the N^* (1700) is striking and irreconcilable. The experiments break into two categories in this regard — either consistent with no decay into Δ (1236) π or a roughly 70% $\frac{\Delta\Delta^{++}\pi^-}{p\pi^+\pi^-}$ branching ratio. The problem is complicated by the fact that the Δ (1236) takes up a large fraction of the Dalitz plot for the Decay of a mass 1700 *MeV* object into $p\pi^+\pi^-$ — a band corresponding to plus and minus a full width covers about 60% of the area of the Dalitz plot. A further complication arises from the fact

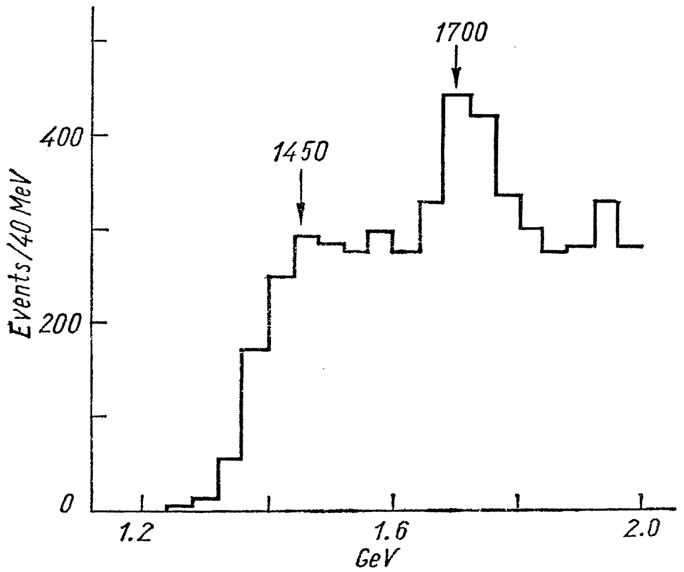

Fig. 25. Combined $p\pi^+\pi^-$ invariant mass plot [61, 62, 63].

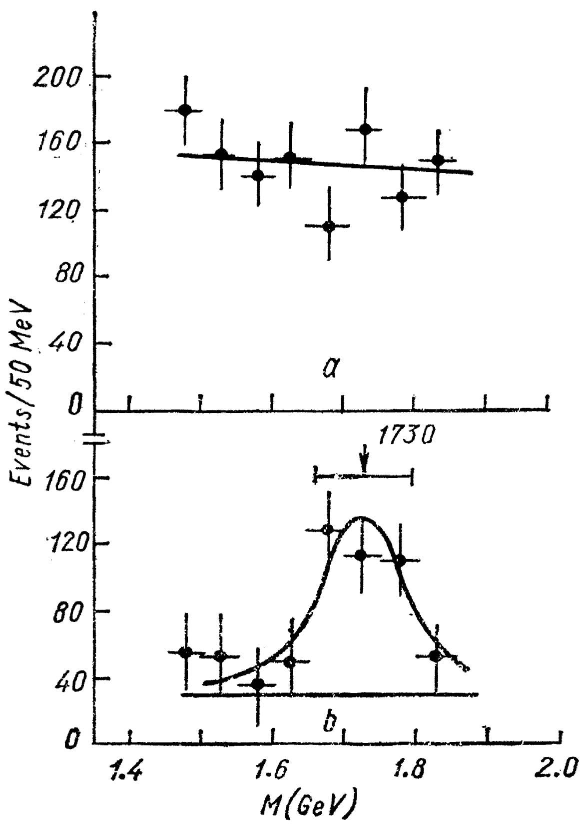

Fig. 26. (*a*) The $\Delta^{++}\pi^-$ component of the $p\pi^+\pi^-$ mass spectrum from $\pi^-p \to \pi^-p\pi^+\pi^-$ at 6 *GeV/c*; (*b*) The non-$\Delta^{++}\pi^-$ component of the $p\pi^+\pi^-$ mass spectrum. David J. Crennell et al. [54].

that a mass cut around the N^* (1700) will typically include more than 70% background. In addition, interference effects are clearly possible and will certainly have to be carefully taken into account before the problems are fully resolved.

Perhaps the most impressive evidence for the N^* (1700) not decaying to Δ (1236) π is shown in Fig. 26 [54]. The $p\pi\pi$ mass spectrum from $\pi^- p \to \pi^- p \pi^+ \pi^-$ at 6.0 GeV/c was broken up into 50 MeV bins and each resulting Dalitz plot fitted with a Breit — Wigner for the Δ (1236) plus a uniform background. As shown in Fig. 26, the amplitude of the Breit — Wigner term is essentially constant across the 1700 MeV region whereas the background amplitude shows a bump of magnitude consistent with the 1730 enhancement in the overall $p\pi\pi$ mass spectrum. A similar result is illustrated in Fig. 27 where a prominent N^* (1700) bump is reduced to a possible shoulder by selecting on a narrow Δ (1236) band. A detailed maximum likelihood fit to this data including the Δ (1236) decay angular distribution yields an upper limit of 8% for the Δ^{++} (1236) $\pi^-/p\pi^+\pi^-$ branching ratio. As shown in Table IV, all groups [52, 53, 54, 55, 58] with most events produced at beam momentum below 10 GeV/c are consistent with no N^* (1700) decay to Δ (1236) π.

Conversely, all groups with beam momenta mainly above 10 GeV/c are consistent with about 70% branching ratio [57, 61, 62, 63]. This result is perhaps best illustrated in Figure 28 from the Purdue group [61] studying the reaction $\pi^+ p \to \pi^+ p \pi^+ \pi^-$ at 13.1 GeV/c. Fig. 28a shows the unselected $p\pi\pi$ mass spectrum as well as (shaded) those events with $1.16 < M\ (p\pi^+) < 1.28$ VeG, for which N * (1700) bump remains prominent. Fig. 28c shows the result of an analysis similar to that described above [54, 55] and exhibits a bump in the $p\pi^+\pi^-$ mass distribution when the Δ (1236) π^- component is plotted. In complete disagreement with lower energy work a Δ (1236) π branching ratio of $75 \pm 15\%$ is quoted [61]. Similar results using similar techniques were obtained by the ABBCHLV collaboration [57] ($75 \pm 15\%$) and a Notre Dame group [68] ($69 \pm 14\%$). Less detailed analyses give Δ (1236) π branching ratios consistent with zero in $K^- p$ interactions at 4.2 GeV/c [52], $\pi^+ p$ at 5.0 GeV/c [53] and $\pi^- p$ mainly at 7.0 GeV/c [58] and consistent with a large branching ratio in $\pi^\pm p$ at 16.0 GeV/c [62]. Older work in $\bar{p}p$ at 5.7 GeV/c [66] and pp at 25 GeV/c [68] is also consistent with a zero branching ratio.

The reason for this seeming inconsistency is not at all clear. It may be simply that the 1700 MeV bump actually consists of a number of resonances with different Δ (1236) π branching ratios whose relative importance varies with the reaction. The $D15$ (1670), $F15$ (1688), $S11$ (1700) and $D33$ (1670) could all be involved. The $D15$ (1670) and $F15$ (1688) both have branching ratios consistent with 70%, whereas the others are unknown [7]. It could also be due to experimental biases or difficulties with the analysis, but the raw data seem too different (see Figs. 27 and 28a) to support this hypothesis. A more probable explanation lies in the possibility of interference between background and resonance decays as may have been indicated by a Rutgers result reported at the Vienna Conference [2] showing a dip in the Δ (1236) component around 1700 MeV. This implies that the N^* (1700) does decay into Δ (1236) π and interferes destructively with the background.

A suggestion has been made by the ABBCHLV collaboration [57] that the N^* (1700) as well as the N^* (1470) is produced by a diffractive mechanism of the type $m + p \to mN^*\pi$, $N^* \to N\pi$. This suggestion is based on the observation that both the 1470 and 1700 MeV enhancements are consistent with being produced via Pomeron exchange as seen by the fact that their production cross

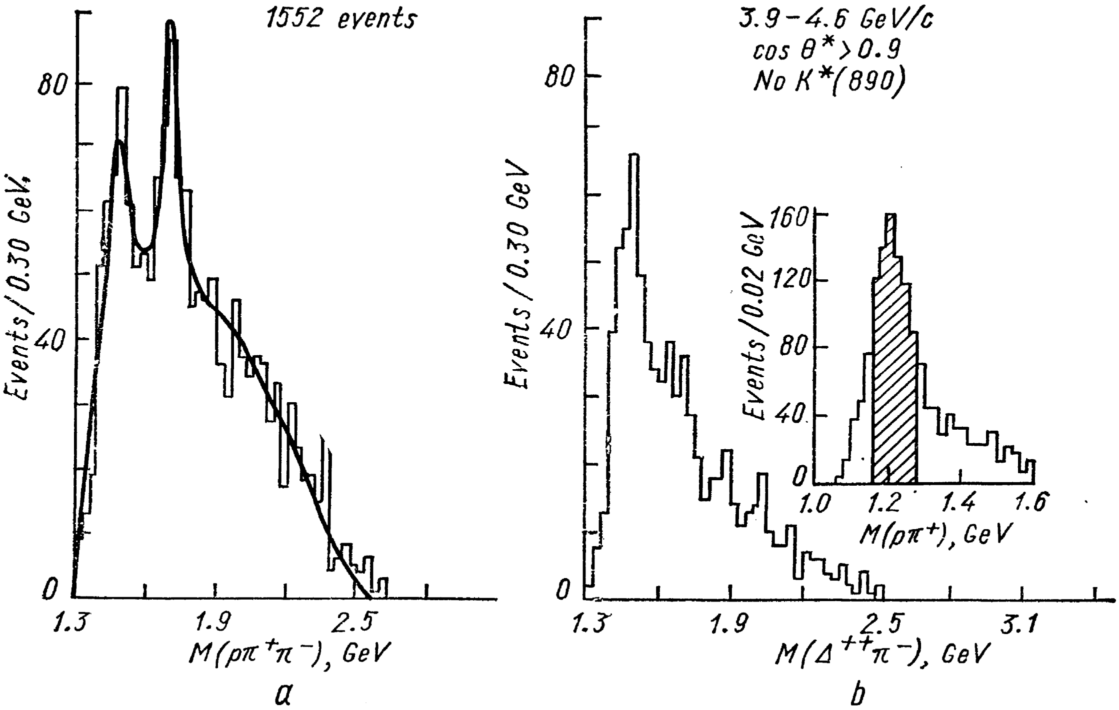

Fig. 27. (*a*) $p\pi^+\pi^-$ mass spectrum from $K^-p \to K^-p\pi^+\pi^-$ at 3.9 and 4.6 *GeV/c* excluding $820 < M\ (K^-\pi^+) < 980$ *MeV* and selecting on production angle θ^* between incident and outgoing K^- so that $\cos\theta^* > 0.9$. (*b*) Same as (*a*) but with selection on a narrow Δ^{++} — $1.16 < M\ (p\pi^+) < 1.28$ *GeV*, as indicated in the insert. V. E. Barnes et al. [55].

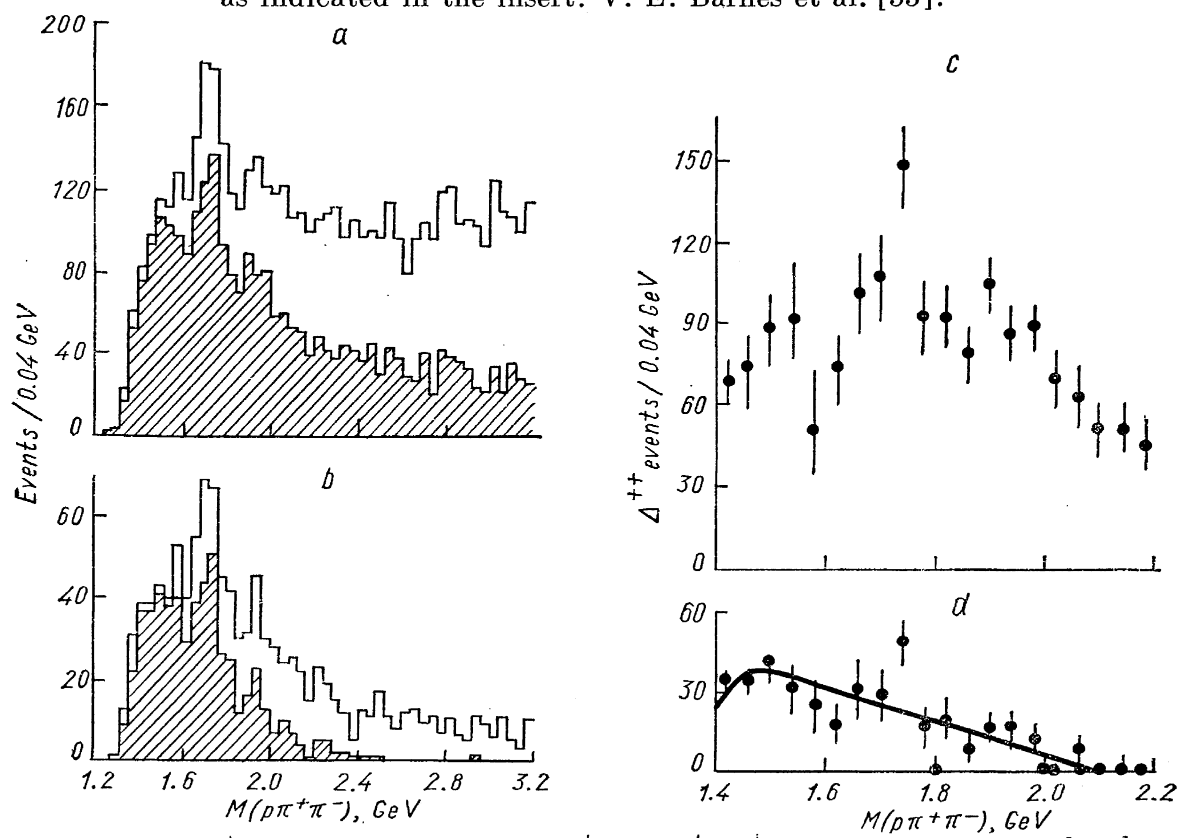

Fig. 28. (*a*) $p\pi^+\pi^-$ mass spectra from $\pi^+p \to \pi^+p\pi^+\pi^-$ at 13.1 *GeV/c*. The shaded histogram contains events with $1.136 < M\ (p\pi^+) < 1.336$ *GeV*. (*b*) Same as (*a*) for a «clean» sample of events for which the angle between the π^- and π_a^+ in the $p\pi_b^+\pi^-$ rest system is greater than 90°. This sample eliminates boson resonance production which is background to the channel of interest here. (*c*) Number of Δ^{++} events vs $M\ (p\pi^+\pi^-)$ obtained by maximum likelihood fits to the $p\pi^+\pi^-$ Dalitz plots. (*d*) Same as (*c*) for the «clean» sample. R. B. Willmann et al. [61].

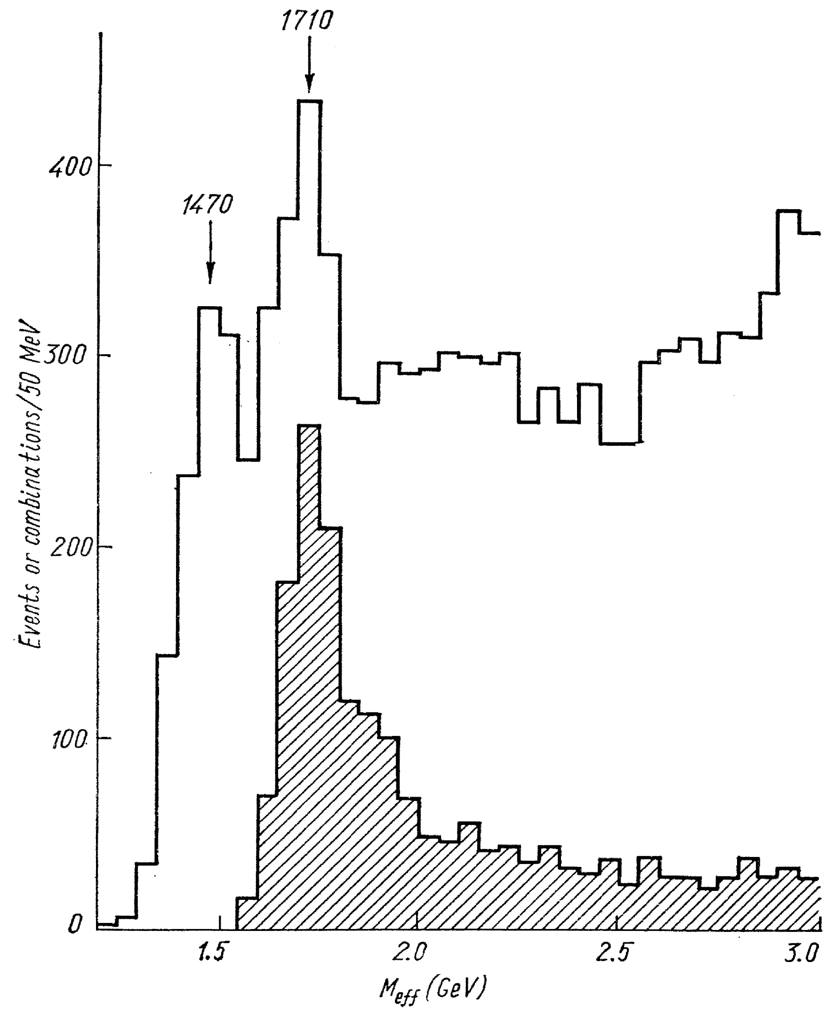

Fig. 29. $p\pi^+\pi^-$ mass spectrum from reactions of the form $mp \to$ $\to mp\pi^+\pi^-$. The shaded area corresponds to events with $p\pi^-$ in the N^{*0} (1470) mass band. K. Boesebeck et al. [57]. Combined distribution from 16 *GeV/c* $\pi^{\pm}$, 10 *GeV/c*. K^-, 8 *GeV/c* π^+.

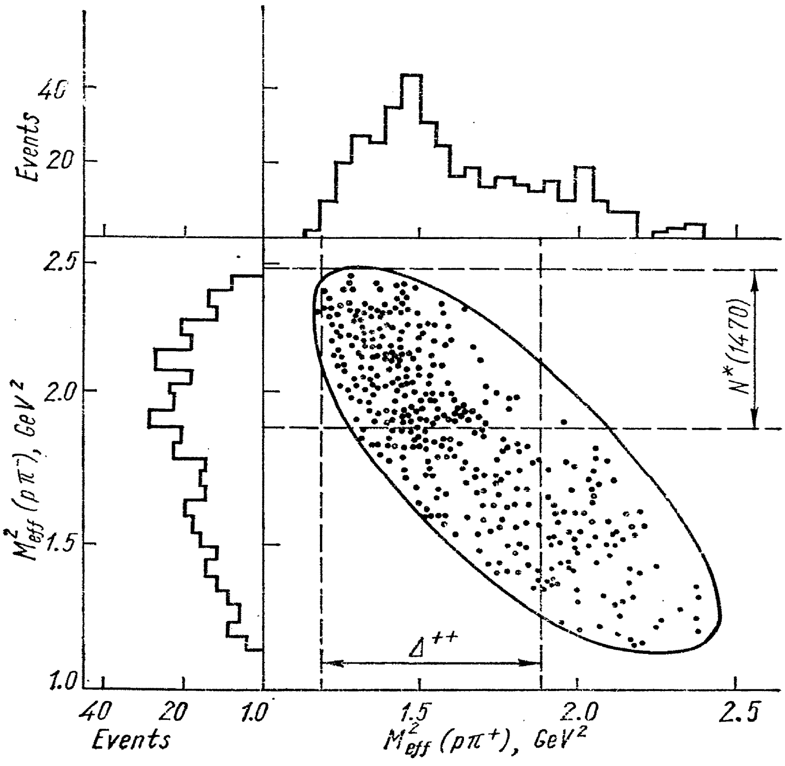

Fig. 30. Dalitz plot of M^2 $(p\pi^+)$ versus M^2 $(p\pi^-)$ for events from the reaction $K^-p \to K^-p\pi^+\pi^-$ at 10 *GeV/c* with M $(p\pi^+\pi^-)$ in the 1710 *MeV* mass band. K. Boesebeck et al. [57].

sections in reactions of the type $mp \to mN^*$ are independent of energy and that they are not produced in the reaction $K^-p \to (n\pi^+\pi^-) K^0$ where charge would have to be exchanged. This is in disagreement with most other investigators who conclude that these bumps are consistent with normal resonance production.

The N^* (1470) is then explained [57] in analogy to the A region in π reactions and the Q region in K reactions as a diffraction dissociation peak in the Δ^{++} (1236) π^- system at low masses in the reaction $m+p \to \Delta^{++}$ (1236) $\pi^- + m$. This would not explain the N^* (1700) due to its being well above the Δ^{++} (1236) π^- threshold. It is then postulated that the N^* (1700) may be due to the reaction $m + p \to N^{*0}$ (1470) $\pi^+ + m$ as a similar threshold effect. The evidence for this conjecture is summarized in Fig. 29, which shows a sharp peak in the $p\pi^+\pi^-$ mass distribution at a mass of 1700 MeV when the $p\pi^-$ mass is selected to be in the N^* (1470) mass band. A peak is, however, kinematically expected as threshold is at about 1600 MeV for the N^* (1470) π system and the probability for the $p\pi^-$ system to lie in the N^* (1470) band decreases as the $p\pi^+\pi^-$ mass increases. An attempt to clarify the question was made by preparing a Dalitz plot for the $p\pi^+\pi^-$ masses in the 1700 MeV region as shown in Fig. 30. Unfortunately, the Δ^{++} (1236) and N^{*0} (1470) mass bands cross in the most populated region of the Dalitz plot and no clear N^{*0} (1470) signal is visible. If true, this hypothesis could explain the variation in the Δ^{++} (1236) π branching ratio of the N^* (1700) as due to varying interferences between the Δ^{++} (1236) and N^{*0} (1470) decay modes.

An angular momentum analysis was attempted by the Purdue group [61] assuming the decay mode N^* (1720) $\to \Delta^{++}\pi^- \to p\pi^+\pi^-$ for the mass region $1620 < M < (p\pi^+\pi^-) < 1820\, MeV$. A maximum likelihood fit was made to the sequential decay assuming $J = {}^3/_2$, ${}^5/_2$, and ${}^7/_2$ to determine the helicity

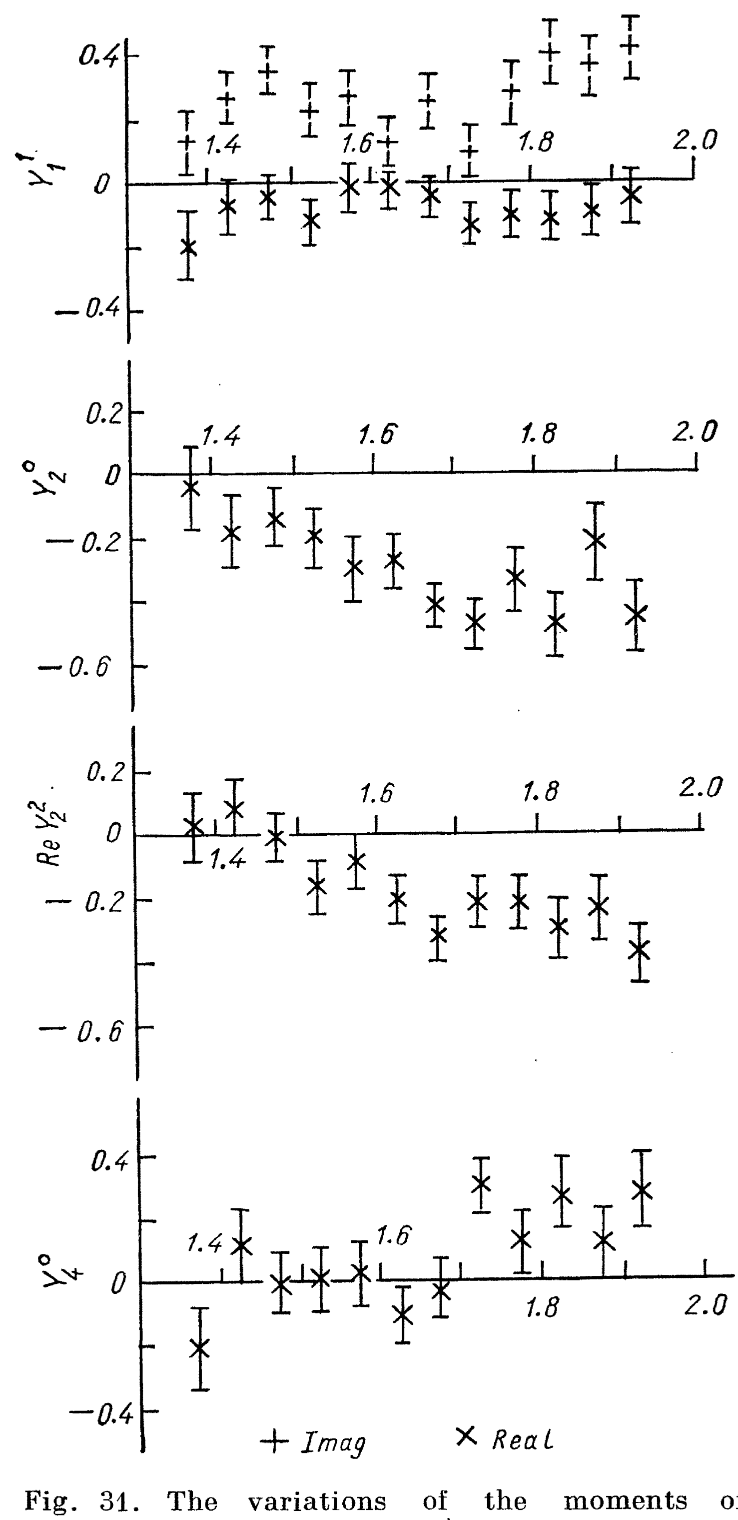

Fig. 31. The variations of the moments of $Y_j^m(\theta, \Phi)$ as a function of $p\pi^+\pi^-$ mass in 50 MeV bins for events from the reaction $K^+p \to K^+p\pi^+\pi^-$ at 10 GeV/c. Birmingham — Glasgow — Oxford Collaboration [56].

amplitudes and the density matrix of the N^* (1720). This procedure rejects $J = {}^3/_2$ on the 10^{-4} confidence level and is consistent with $J = {}^5/_2$ and ${}^7/_2$ although the neglect of the large background under the N^* (1720) makes this conclusion uncertain.

A detailed partial wave analysis of the $p\pi^+\pi^-$ system below 1750 *MeV* was carried out by a Birmingham — Glasgow — Oxford collaboration [56] using 7067 examples of $K^+p \to K^+p\pi^+\pi^-$ at 10 *GeV/c*. This is a preliminary result and will be extended using over 11.000 events. The $p\pi^+\pi^-$ system was assumed to be produced at the target proton vertex and a cut was made restricting momentum transfer to < 0.5 $(GeV/c)^2$. In addition the K^{*0} (890) was removed ($830 <$ $< M$ $(K^+\pi^-) <$ 950 *MeV*). This cut data shows clear peaks at 1480 and 1690 *MeV*.

A model independent fit was made to the angular distribution of the target proton in the $(p\pi^+\pi^-)$ center of mass system taking the axis as perpendicular to the $(p\pi^+\pi^-)$ plane and the X axis along the π^- direction. The major results as indicated in Fig. 31 are (I) Im Y_1^1 is large indicating at least two waves of opposite parity in the entire mass region, (II) Y_2^0 is appreciable above about 1450 *MeV* indicating the presence of waves with $J \geqslant {}^3/_2$, (III) Y_4^0 is significant around 1700 *MeV* indicating waves with $J \geqslant {}^5/_2$.

A model dependent fit to all characteristics of the events was also attempted

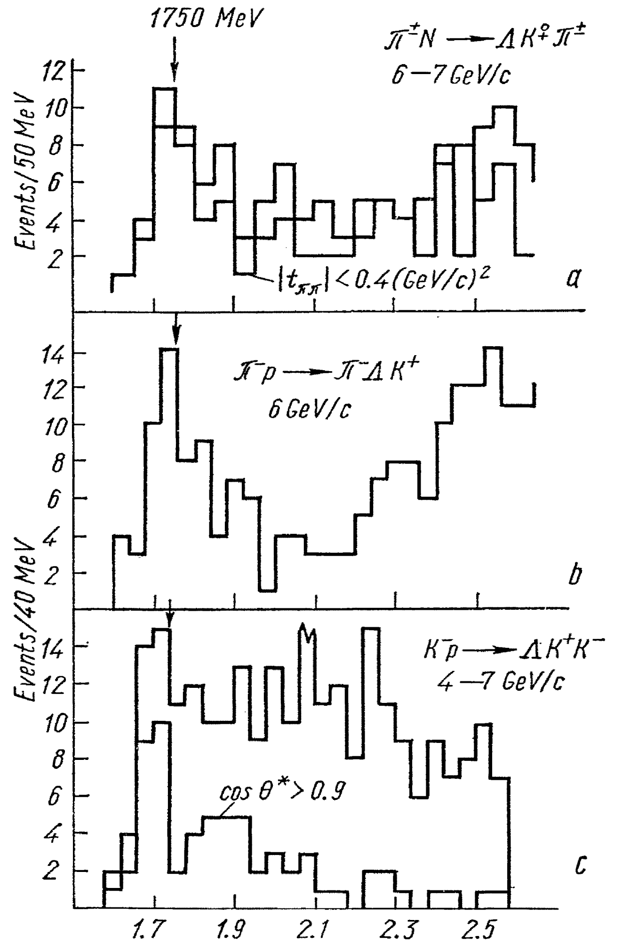

Fig. 32. Evidence for the decay mode N^* (1700) $\to \Lambda K$. (*a*) R. Morse et al. [58]. (*b*) David J. Crennell et al. [54]. (*c*) V. E. Barnes et al. [55].

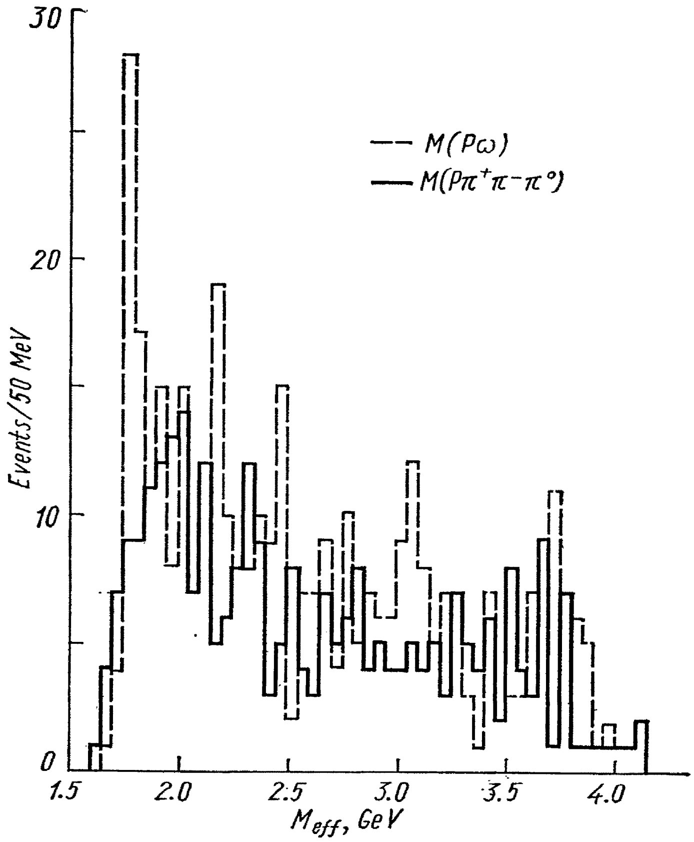

Fig. 33. Evidence for the decay mode N^* (1700) $\to p\,\omega$ in the reaction $pp \to pp\pi^+\pi^-\pi^0$ at 13.1 *GeV/c*. The dotted curve corresponds to $725 < M$ $(p\pi^+\pi^-\pi^0) < 825$ *MeV* — the ω region — and the full curve to $650 < M$ $(\pi^+\pi^-\pi^0) <$ < 900 *MeV* excluding the ω band. J. Le Guyader et al. [60].

assuming the $(p\pi\pi)$ system decays into Δ (1236) π and $p\sigma$ in the $J^P = {}^1/_2{}^+$ wave, where σ is an s wave $\pi\pi$ interaction. Limitations in this formulation include the neglect of $p\rho$ amplitudes which may be important for the upper mass range and the neglect of non Δ (1236) π contributions which may be due to other than $J^P = {}^1/_2{}^+$ waves going into a $p\sigma$ state. These approximations probably limit the usefulness of the fit to the region below 1600 *MeV*. The major results of the fit are (I) the ${}^1/_2{}^+$ wave is large in the 1500 *MeV* region and exhibits comparable coupling to Δ (1236) π and $p\sigma$ states. (II) the ${}^3/_2{}^-$ wave is large from threshold, (III) the ${}^5/_2{}^+$ wave is small until 1600 *MeV* and then becomes important. (IV) ${}^1/_2{}^-$ and ${}^5/_2{}^-$ waves are not needed. These results are in general agreement with the presence of the *P*11 (1470), *D*13 (1520), *F*15 (1688), and *P*11 (1780) resonance expected from the elastic phase shift analysis.

Recent data on the branching ratio of the N^* (1700) into ΛK are summarized on Fig. 32. A positive signal is observed by the Wisconsin — Toronto group (Fig. 32*a*) [58], and numerical branching ratios have been published by two Brookhaven groups — 5 ± 1% (Fig. 32*b*) [54] and 4 ± 1.5% (Fig. 32*c*) [55]. Negative, but not really contradictory results have been obtained with limits <4% [53], < 2.5% [61] and < 2% [66]. All errors and limits are on the one standard deviation level. The reactions and energies are summarized in Table IV.

A strong indication for decay into $p\omega$ but not into uncorrelated $p\pi^+\pi^-\pi^0$ by the N^* (1700) is shown in Fig. 33 [60]. The peak, which has a mass of 1750 ± 25 *MeV* and width 100 ± 25 *MeV* is consistent with the N^* (1700) within 2.5 standard deviations as well as with a previous observation [69].

B. Miscellaneous N^* Contributions. Azimov [70] has postulated the possible existence of a new nucleon state probably below the $N\pi$ threshold which could be observed by the decay mode $N' \to N\gamma$. This is based on a possible new octet containing the Ξ (1630), Σ (1475) and Λ (1330), none of which are yet firmly established [7]. It could be observed in production experiments using the $N\gamma$ decay mode or in missing mass experiments which already put a limit of 50 μb [71]. Other possibilities for detection include electroproduction experiments and π^- capture in hydrogen.

A $N\pi\pi$ decay mode of the *G*17 (2190) was reported with good statistics [57]. The reported mass 2203 ± 10 *MeV* and width 175^{+120}_{-50} are both consistent with the parameters obtained with large errors from the elastic phase shift analysis. In addition, evidence for a N^* (1300) was reported by this group.

Weak evidence for two $p\eta$ decay modes of nucleon resonances was presented using the reaction $\bar{p}p \to \bar{p}pX^0$ at 6.9 *GeV* (as shown in Fig. 34 [72]). The quoted parameters are (1570 ± 20, 90 ± 45) and (1865 ± 30, 150 ± 60) for the (mass, width) of the two resonances. A new method of analysis called the «mass variation method»

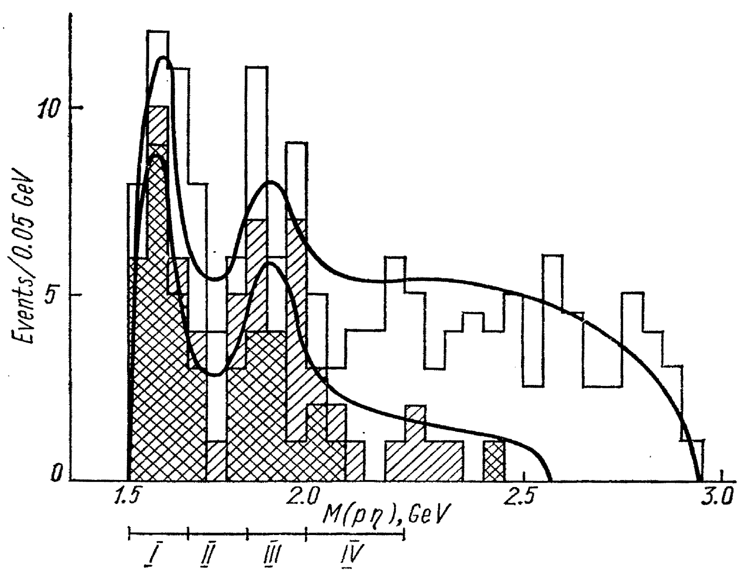

Fig. 34. $p\eta$ mass spectra from the reaction $\bar{p}p \to \bar{p}p\eta$ at 6.9 *GeV/c*. The single hatched histogram is for events with $|t| < 0.35$ $(GeV/c)^2$ and the double hatched also restricts the $\bar{p}\eta$ mass to 1.5 — 2.0 *GeV*. T. Kitagaki et al. [72].

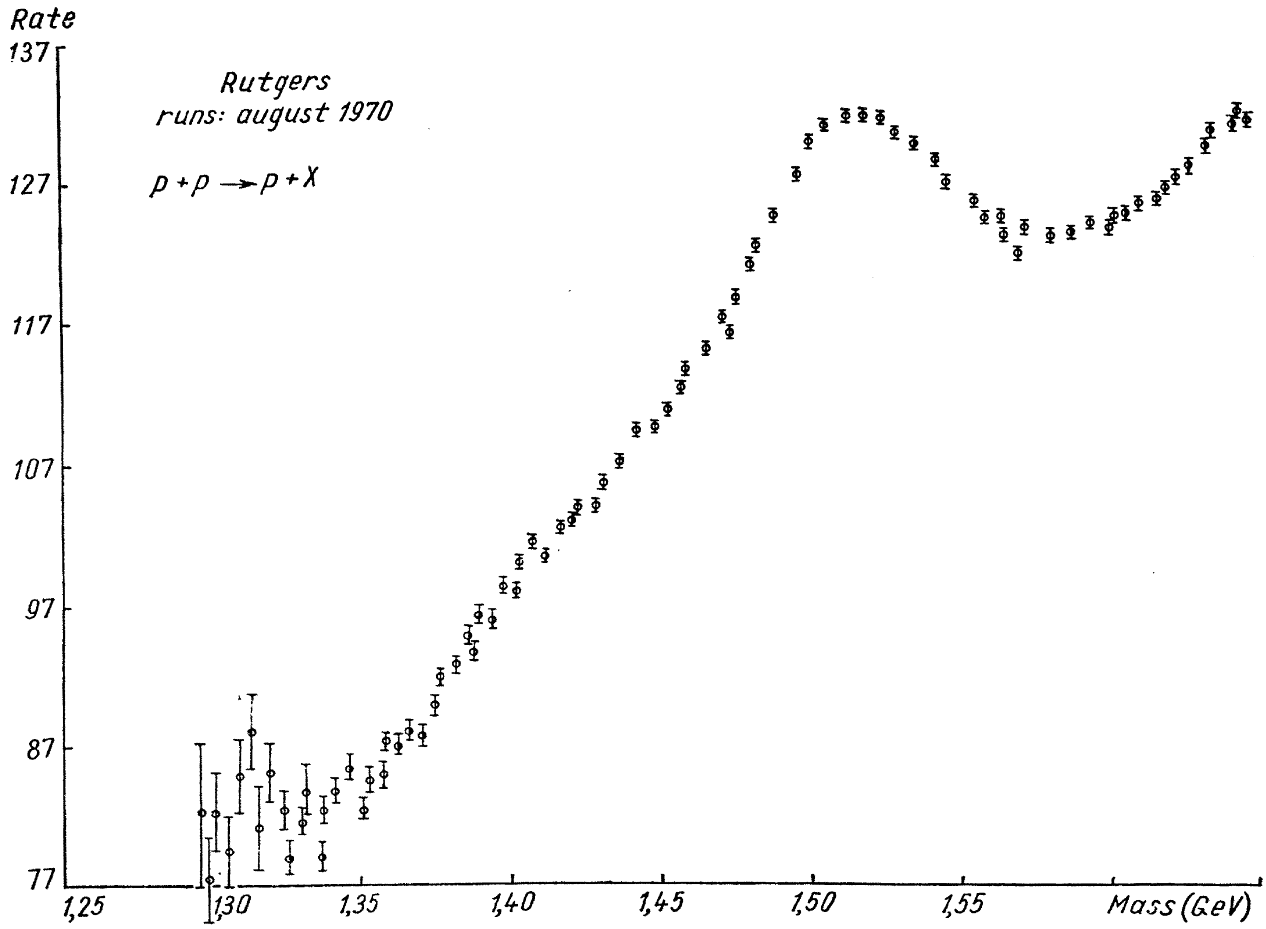

Fig. 35. Missing mass spectrum in the region of the N^* (1520). Note the suppressed zero on the vertical scale. F. Sannes et al. [74].

[73] was used to improve the signal to noise ratio — a very important consideration in experiments of this type where 156 events were called from 8.6 *K* measurements using missing mass techniques. Rapid changes in the *t* distribution and other angular distributions give supporting evidence to the rather weak evidence in the mass plot. Although the statistics are as yet quite poor, the reaction and technique are quite interesting in that they give an opportunity to study pure $I = {}^1/_2$ nucleon states.

The counter group at Rutgers contributed a preliminary report on a search for fine effects in the N^* spectrum [74] (fig. 35). The extremely simple apparatus — a missing mass spectrometer using the reaction $pp \to pX$ — consists of a 2 *cm* liquid hydrogen «point» target, a 60 element hodoscope placed 16 *ft* away to measure the angle precisely, absorbers to measure the proton momentum roughly and time of flight to select on protons. This apparatus, using no computer or magnet, permits gathering of data with a resolution of $\pm$ 5 *MeV* with statistics of about 10^6 events per 2 *MeV* bin per day.

A preliminary run yielded the Δ (1236) with a width of 100 $\pm$ 10 *MeV* and the N^* (1520) with a width of 65 $\pm$ 10 *MeV* in disagreement with the elastic phase shift results of 105 to 150 *MeV* [7]. A search for previously unobserved resonances on the 1% level is now in progress.

IV. Summary

Although the experimental status of the non-strange baryon resonances has not changed in any fundamental way since the Vienna Conference [1, 2], a large amount of detailed and difficult experimental data gathering and analysis has been carried out which has improved and sharpened previous numbers and conclusions. This work has served to improve confidence in previous work and indicated directions for future research.

Recent work on elastic phase shift analysis has strengthened previously definite states and left the weak states relatively undertain. One important addition is the recognition of two new H wave resonances [31] — the $H3$, 11 (2320) and $H19$ (2220) which are consistent with being Regge recurrences of the $F37$ (1950) and $F15$ (1690) respectively.

More precise information on YK and $N\eta$ channels is very much needed as well as detailed information at higher energies to constrain the elastic branching ratios and to push the elastic phase shift analyses to higher mass values.

The information from three body channels in formation experiments is increasing and reaching the level at which it can appreciably complement the two body channels. However, there remain severe problems with the isobar and other models needed to analyze this data and great care is needed.

If fundamentally useful information is to be obtained from production experiments, more data and, most critically, more detailed analyses are needed. In particular, complete fits including resonance and background effects in a coherent manner are essential to determine which partial waves and decay modes are contributing at each mass value.

Acknowledgements

I would like to thank the Scientific Secretaries associated with this report for their devoted hard work and other contributions. I am especially grateful to the discussion leaders, John Mulvey and Sandy Donnachie, with whom I very much enjoyed working and who are responsible for most of the good ideas in this report.

DISCUSSION

M o r a v c s i k: I have three remarks about partial wave analysis.

The first two pertain to going to higher energies. This is important because we want to know if resonances continue to occur at arbitrary energies or not.

1. One should use the Cutkosky — Deo — Ciulli parametrization, since it can give a representation in terms of fewer parameters than the usual partial wave decomposition.

2. The phase band method makes the assumption that if one has many angular momentum states, one can determine each parameter almost independently of the others, just like we can determine a Fourier coefficient in the decomposition or a function independently of the other coefficients. This is not in conflict with the possible existence of individual correlations among partial wave parameters, just as there may be correlations between independently determined Fourier coefficients. Furthermore the method is a selfconsistent one and hence the assumption is **a posteriori** checked.

One should combine the Cutkosky — Deo — Ciulli parametrization with the phase band method for the best results at high energies.

I would like to appeal therefore for experiments for **complete** angular distributions of differential cross section **and** polarization at some high energy (e.g. 5 GeV or 10 GeV). The method of analysis is ready.

3. One should now **drop** the quasi-two-body assumptions in $\pi N \to \pi\pi N$ analyses and do a complete three body partial wave analysis. This would avoid double counting and would give information on the crucial question of to what quantitative extent the quasi-two-body mechanism is supplemented by uncorrelated three-body final states.

Y o k o s a w a:

I would like to make 2 comments on the phase-shift analysis up to 2.80 GeV/c.

1. Our preliminary analysis up to 2.8 GeV/c at ANL strongly indicate necessity of higher partial waves than H-wave, namely, I- and possibly J-waves. However, if we include the two more waves, one cannot reach unique solution because of too many parameters.

2. Our recent π^+p polarisation data up to 2.30 GeV/c are in serious disagreement with the currently available phase-shift analyses.

In views of the above two points, how much one can trust those two new resonances, H_{19} (2220) and $H_{3.11}$ (2420)?

P l a n o:

I believe the disagreement with the recent polarization data is not serious in that the general features of the data are followed by the phase shift prediction. A new fit, which is certainly called for, will I believe fit the new data without changing the resonance parameters greatly. If higher partial waves than H were not included, the reliability of the H resonances is indeed somewhat questionable, but I believe at least I-waves were included.

M i c h e j d a:

I have a comment on the comparison of the data from the N^* production experiments and the results of the phase-shift analysis. Some 3 years ago when first data on production of higher isobars became available they were ignored by the phase-shift people. It is true that they were scarce and not very significant.

Now the situation has changed. There is quite a lot of good data from various reactions and at various energies. Let us consider an example of 1700 MeV peak which is observed in production as having narrow width of about 60 MeV. The phase shift analyses give resonances in this mass region with the widths equal or larger than 120 or 140 MeV. I wonder what is the opinion of the phase shifts experts about this situation.

Should there not be at least one narrow resonance in this region?

P l a n o:

There may indeed be a narrow resonance in this region. However it is notoriously difficult to extract accurate resonance widths from phase shift analysis because of the uncertainties of the background. The usual assumption is that the background is slowly varying compared to the resonance, but if this is not true (and at the moment there is no way of knowing) then the extracted resonance widths could be appreciably narrower than are at present quoted. It would be extremely useful if production experiments were capable of specifying the quantum number of this 1700 MeV peak.

K e n n e y:

I have a correction and a comment on the decay of N^* (1700) $\to \Delta\pi$. The correction: our branching ratio determination was based on a different data sample (combined 18.5 GeV/c $\pi^{\pm}p$, 8 GeV/c π^-p) than that of the M $(p\pi\pi)$ plot shown, and is not in disagreement with the M $(p\pi\pi)$ for the combined sample. The comment: we have studied the question of the dependence of the branching ratio on the background of non-resonant $\Delta\pi$ assumed and the disagreement between the BNL result and that of the groups that find $\sim 70\%$ $\Delta\pi$ decay can probably be understood in terms of the uncertainty in the $\Delta\pi$ background.

F i o r i n i:

I have a general comment concerning the role played by baryon resonances in nuclear physics. In a recent paper by Kissinger, for instance, the presence of resonances in deuterium was suggested. Most of the present experiments on baryon resonances are on protons, but it would be interesting to study their effects in nuclei, both for nuclear physics and for elementary particle physics.

Leith:

I would like to make a comment on the disagreements between the various detailed analyses of the spins and branching ratios of $N\pi\pi$ resonances seen in production mode. We know that this region is very complicated, containing resonances in, at least, the following partial waves: D, F, P and S. Each of these states is produced with its own production mechanism which depends on the energy of the experiment and on the nature of the incident particle. Therefore, the portion of each of these resonances presenting in the $N\pi\pi$ mass spectrum near 1700 MeV will change with energy and experiment. We must therefore expect analysis of the spin composition and of the branching ratio to change with the energy and nature of the incident particle.

Hughes:

Concerning the determination of branching ratios of N^* from production experiments I believe that in a complicated situation like that which exists the only satisfactory method is to analyse either the whole process or at least the Dalitz plot as a function of $p\pi\pi$ mass.

REFERENCES

1. A. Donnachie, Proceedings of the Fourteenth International Conference on High Energy Physics, Vienna, Austria, September, 1958. Edited by J. Prentki and J. Steinberger (CERN Scientific Information Service, Geneva, Switzerland, 1968), p. 139.
2. J. G. Rushbrooke, idem, p. 158.
3. R. J. Plano, Proceedings of the Lund International Conference on Elementary Particles, Lund, Sweden. Edited by G. von Dardel (Berlingska Boktryckeriet, Lund, Sweden, 1969), p. 323.
4. C. Lovelace, Proceedings of the International Conference on Elementary Particles, Heidelberg, Germany, 1967. Edited by H. Filthuth (North Holland Publishing Company, Amsterdam, The Netherlands, 1967) p. 79.
5. R. P. Feynman, S. Pakvasa and S. F. Tuan, University of Hawaii Preprint UH—511—64—70 (April, 1970).
6. I would especially like to thank Claud Lovelace, A. T. Lea, Art Rosenfeld, John Mulvey and A. Donnachie for valuable discussions.
7. Particle Data Group, Physics Letters **33B**, 1 (August, 1970).
8. A. A. Carter, J. R. Williams, D. V. Bugg, P. J. Bussey and D. R. Dance, Preprint (July, 1970).
9. K. Wendell Chen et al., Paper 5a—2.
10. M. G. Albrow et al., Paper 5a—14.
11. R. M. Brown et al., Paper 5a—5.
12. G. Burleson et al., Paper 1c—2.
13. J. M. Abillon et al., Paper 5a—3.
14. A. D. Brody et al., Paper 5a—13.
15. G. E. Kalmus et al., Paper 1a—26.
16. R. Socolow, Thesis, Harvard University, 1964, Unpublished.
17. Norman E. Booth, Phys. Rev. Letters **21**, 465 (1968).
18. R. Ayed, P. Bareyre and G. Villet, Physics Letters **31B**, 598 (1970).
19. R. K. Roychoudhury, R. Perrin and B. H. Bransden, Nuclear Physics **B16**, 461 (1970).
20. C. M. Johnson and H. M. Steiner, UCRL Report 18001.
21. A. Donnachie, R. G. Kirsopp and C. Lovelace, Physics Letters **26B**, 161 (1968).
22. A. T. Davies and R. G. Moorhouse, Nuovo Cimento **52A**, 1112 (1967) and Vienna Conference.
23. D. J. Herndon, A. Barbaro-Galtieri and A. H. Rosenfeld, UCRL 20030 (February, 1970).
24. V. Barger and R. J. N. Phillips, Phys. Rev. **187**, 2210 (1969).
25. P. J. Duke, D. P. Jones, M. A. R. Kemp, P. G. Murphy, J. D. Prentice and J. J. Thresher, Phys. Rev. **149**, 1077 (1966).
26. J. A. Helland, T. J. Devlin, D. E. Hagge, M. J. Longo, B. J. Moyer and C. D. Wood, Phys. Rev. **134B**, 1062 (1964) and Phys. Rev. **134B**, 1079 (1964).
27. D. M. Ogden, D. E. Hagge, J. A. Helland, M. Banner, J. F. Deteouf and J. Leiger, Phys. Rev. **137B**, 115 (1965).
28. P. Bareyre, C. Bricman and G. Villet, Phys. Rev. **165**, 1730 (1968).

29. C. H. Johnson, UCRL Report 17683 (1967).
30. G. E. Kalmus, G. Borreani and J. Louie, UCRL Report 19735 (March, 1970), Submitted to Phys. Rev.
31. R. Ayed, P. Bareyre and G. Villet, Paper 5a—9.
32. G. C. Wrighton et al., Paper 11a—17.
33. David Bridges et al., Paper 5a—6.
34. D. Bridges, M. J. Moravcsik and A. Yokosawa, Phys. Rev. Letters **25**, 770 (1970).
35. M. M. Makarov et al., Paper 5a—10.
36. A. V. Kravtsov, Paper 5a—7.
37. D. H. Saxon, J. H. Mulvey and W. Chinowsky, Oxford University Preprint (March, 1970).
38. P. Chavanon et al., Part II, Paper 5a—8.
39. Nguyen Thuc Diem et al., Part I, Paper 5a—8.
40. A. D. Brody et al., Paper 2a—11.
41. U. Mehtani et al., Paper 5a—11.
42. J. M. Namyslowski, M. S. K. Razmi, R. G. Roberts, Phys. Rev. **157**, 1328 (1967). G. C. Wick, Ann. Phys. **18**, 65 (1962).
43. V. A. Schegelsky, Preprint FTI—165, Leningrad (1969).
44. J. P. Baton, G. Laurens and J. Reignier, Nuclear Phys. **B3**, 349 (1967).
45. M. De Beer et al., Nuclear Phys. **B12**, 599 (1969).
46. P. Eberhard and M. Pripstein, Phys. Rev. Letters **10**, 351 (1963).
47. Y. Williamson et al., Paper 5a—12.
48. L. P. Glonti et al., Paper 1c—5.
49. S. I. Bilenkaya et al., Paper 5a—4.
50. L. N. Glonti, Yu. M. Kazarinov, A. M. Rozanova and I. N. Silin, Jadernaya Fizika **7**, 1060 (1968).
51. A. Pazman, S. I. Bilenkaya, J. Bystricky, Z. Janout, Yu. M. Kazarinov and F. Lehar, Czech, J. Phys. **B19**, 882 (1969).
52. Nijmegen — Amsterdam Collaboration, Paper 5b—7.
53. Bonn — Durham — Nijmegen — Paris (E. P.) — Torino Collaboration, Paper 5b—3.
54. David J. Crennell, Kwan Wu Lai, James Louie, J. Michael Scarr and W. H. Sims, Phys. Rev. Letters **25**, 187 (1970).
55. V. E. Barnes, D. Bassano, S. U. Chung, R. L. Eisner, E. Flaminio, J. B. Kinson and N. P. Samios, Phys. Rev. Letters **23**, 1516 (1969).
56. Birmingham — Glasgow — Oxford Collaboration, Paper 5b—5.
57. K. Boesebeck et al., Paper **5b—9.**
58. R. Morse et al., Paper 5b—10.
59. P. Antich et al., Paper 3b—4.
60. J. Le Guyader et al., Paper 3a—21.
61. R. B. Willmann, J. W. Lamsa, J. A. Gaidos and C. R. Ezell, Phys. Rev. Letters **24**, 1260 (1970).
62. J. Ballam et al., Paper 12—24.
63. P. H. Smith et al., Paper 5b—4.
64. A. P. Gasparyan et al., Paper 5b—6.
65. K. F. Galloway, E. D. Alyea Jr., R. R. Crittenden, W. F. Prickett and H. J. Martin, Physics Letters **27B**, 250 (1968).
66. V. Alles—Borelli, B. French, A. Frisk and L. Michejdá, Nuovo Cimento **47**, 232 (1967).
67. R. A. Jespersen, Y. W. Kang, W. J. Kerman, R. A. Leacock, J. I. Rhode, T. L. Schalk and L. S. Schroeder, Phys. Rev. Letters **21**, 1368 (1968).
68. R. Ehrlich, R. Nieporent, R. J. Plano, J. B. Whittaker, C. Baltay, J. Feinman, F. Franzini, R. Newman and N. Yeh, Phys. Rev. Letters **21**, 1839 (1968).
69. M. S. Milgram, S. Vhao, T. F. Johnston, J. Prentice, N. R. Steenberg, T. S. Yoon, R. Morse, B. Y. Oh and W. D. Walker, Nuclear Physics **B18**, 1 (1970).
70. Ya. I. Azimov, Paper 5b—11.
71. E. W. Anderson et al., Phys. Rev. Letters **16**, 855 (1966).
72. T. Kitagaki et al., Paper 5b—1.
73. T. Kitagaki, S. Tanaka, T. Sato, K. Hasegawa, K. Tamai, R. Sugawara, H. Kichimi, T. Okosawa, S. Noguchi, M. Kondo, K. Abe and K. Takahashi. To be published in Phys. Rev.
74. F. Sannes et al., Paper 5b—12.
75. L. D. Roper, R. M. Wright and B. T. Feld, Phys. Rev. **138**, B190 (1965).